FABRICATION OF THIOL REACTIVE POLYMERIC MICROSTRUCTURES

by

Tuğçe Nihal Gevrek

B.S., Chemistry Education, Marmara University, 2008

Submitted to the Institute for Graduate Studies in
Science and Engineering in partial fulfillment of
the requirements for the degree of
Master of Science

Graduate Program in Chemistry

Boğaziçi University

2011

FABRICATION OF THIOL REACTIVE POLYMERIC MICROSTRUCTURES

APPROVED BY:

Assoc. Prof. Amitav Sanyal (Thesis Supervisor)	……...
Assist. Prof. Rana Sanyal	……
Assist. Prof. Şenol Mutlu	……

DATE OF APPROVAL: ……...

To my family

ACKNOWLEDGEMENTS

I would like to express my sincere gratitude to my thesis supervisor Assoc. Prof. Amitav Sanyal for his endless attention and scientific guidance throughout this study. I appreciate his support and useful comments throughout my laboratory work.

I would extend my thanks to Assist. Prof. Rana Sanyal for accepting me to their research group and for her efforts to provide a productive research environment.

I wish to express my appreciation to Assist. Prof. Senol Mutlu for his support and guidance in micropatterning studies and optical microscope.

I would like to extend my thanks to Assist. Prof Stefan Fuss, for his help in using fluorescence microscope.

I would like to express my gratitude to Eun Ju Park for her endless help in this project and also for her enjoyful friendship and İrem Kosif for helping me to be a member of this research group and her endless patience. I would like to thank to Merve Coşar, Hasan Can Helvacı, Şensu Celasun, Rana Nur Özdeslik, Semra Şahin and Yasemin Üzüm for their support, research work and friendship. I also thank my labmates, Özgül Gök, Elif İyilik, Saltuk B. Hanay, Sadık Kağa, Gönül Demirci, Melike Eceoğlu, Nuray Bilgen, Gamze Tanrıver, Betül Demirer, Pelin Ertürk, Nazlı Böke, Özlem İ. Kalaoğlu, Mehmet Arslan, Nergiz Cengiz, Gülen Tonga, Sezin Yiğit, Serap Yapar, E. Ece Geçici, Oyuntuya Munkhbat, Sebla Onbulak, K. Merve Türksoy, Burcu Sümer, Tuğba Genç and Firat Özdemir for their companionship. I would like to thank all the members of the faculty in the Chemistry Department.

This research has been supported by The Scientific and Technological Research Council of Turkey (TUBITAK) (110T068).

ABSTRACT

FABRICATION OF THIOL REACTIVE POLYMERIC MICROSTRUCTURES

PEG-based 3D hydrogel patterns containing thiol reactive maleimide functional groups have been prepared using a novel Diels-Alder/retro Diels-Alder strategy. Bulk-hydrogels and hydrogel patterns containing various amount of thiol reactive maleimide were synthesized by photo-polymerization in presence of photoinitiator and PEG-DA cross linker. The thiol reactive maleimide group was protected with furan during gelation of bulk-hydrogel and patterning of hydrogels and then was deprotected by retro-Diels-Alder reaction. After activation of maleimide in the hydrogel structure, the reactive maleimide group embedded hydrogels can be efficiently derivatized with thiol containing molecules such as a fluorescent dye, BodipyC10SH. Thiol containing biotin derivatives were covalently attached to the thiol reactive maleimide in bulk-hydrogel and hydrogel patterns under mild condition. Immobilization of FITC-streptavidin onto biotinylated hydrogel patterns were performed and investigated by fluorescence microscope. In order to detect amount of accessible biotin in the hydrogel, HABA-assay was carried out with biotinylated bulk-hydrogels.

ÖZET

TİYOL REAKTİF MİKRO DESENLERİN HAZIRLANMASI

Tiyol gruplarına karşı reaktif maleimid foksiyonel grubu barındıran PEG tabanlı 3 boyutlu hidrojel desenler yenilikçi bir Diels-Alder/retro Diels-Alder stratejisi kullaılarak hazırlanmıştır. Çeşitli miktarlarda tiyol reaktif maleimid içeren dökme hidrojeller ve hidrojel desenler fotopolimerizasyon başlatıcı ve PEG-DA çapraz bağlayıcı varlığında fotopolimerizasyon ile sentezlenmiştir. Bulk ve desenlenmiş hidrojellerin sentezi esnasında tiyol reaktif maleimidler furan ile korumuş halde bulunmaktadır ve jelleşme sonrasında retro Diels-Alder reaksiyonu ile koruması kaldırılmıştır. Hidrojeldeki maleimid gruplarının aktifleştirilmesinden sonra, reaktif maleimid grupları tiyol grubu barındıran boya molekülleriyle foksiyonelleştirilebildiği gösterilmiştir. Tiyol grubu barındıran biyotin türevi tiyole karşı reaktif olan maleimid grupları içere bulk ve desenledirilmiş hidrojellere oda koşullarında kovalent olarak bağlamıştır. Biyotilenmiş hidrojel desenlerine FITC-streptavidin sabitlenmesi ise floresan mikroskop ile takip edilmiştir. Hidrojel içerisideki biyotin miktarını tayin etmek için HABA-assay biyotinlenmiş bulk hidrojel ile gerçekleştirilmiştir.

TABLE OF CONTENTS

ACKNOWLEDGMENTS iv
ABSTRACT v
ÖZET vi
LIST OF FIGURES ix
LIST OF TABLES xi
LIST OF ACRONYMS/ABBREVIATIONS xii
1. INTRODUCTION 1
1.1. Hydrogels 1
1.1.1. Functionalizable Hydrogels 3
1.2. Soft Lithography and Microfabrication 7
1.2.1. The tools of Soft Lithography 8
1.2.1.1. Replica Molding (REM) 8
1.2.1.2. Microcontact Printing 9
1.2.1.3. Micromolding in Capillaries 11
1.2.1.4. Microtransfer Molding 13
1.3. Patterned Hydrogels 13
2. AIM OF THE STUDY 15
3. RESULTS AND DISCUSSION 16
3.1. Synthesis of Photopolymerized Bulk-Hydrogel 16
3.2. Thermogravimetric Analysis of Hydrogels 18
3.3. Elemental Analysis of Bulk-Hydrogels 19
3.4. Swelling Study of Bulk-Hydrogel 20
3.5. Morphology Analysis of Bulk Hydrogels 22
3.6. Biotin Concentration Determination 23
3.7. Preparation and Activation of Photopolymerized Hydrogel Pattern 25
3.8. Dye Immobilization on Patterned Hydrogels 26
3.9. Streptavidin Immobilization on the Biotinylated HP 28
4. EXPERIMENTAL 31
4.1. Materials 31

4.2. Fabrication of Photopolymerized Bulk-Hydrogel 31
4.3. Swelling Study of Bulk-Hydrogel 32
4.4. Modification of Silicon Wafer Substrate with TMSPMA 32
4.5. Preparation and Activation of Photopolymerized Hydrogel Pattern 33
4.6. Streptavidin Immobilization on the Biotinylated HP 34
4.7. HABA/Avidin Assay of Biotinylated Bulk-Hydrogel … 34
4.8. Measurement and Characterization 34
5. CONCLUSIONS 36
REFERENCES 37

LIST OF FIGURES

Figure 1.1. Physically crosslinked hydrogels. 2

Figure 1.2. Hydrogel synthesized via click reaction from dendron-polymer-dendron conjugates. 5

Figure 1.3. Thiol reactive hydrogels. 6

Figure 1.4. The fabrication of micropatterned slabs of PDMS. 7

Figure 1.5. Fabrication of micropatterned agarose gels via replica molding. 8

Figure 1.6. Catalysts free Huisgen 1,3-dipolar cycloaddition reaction via micro contact printing technique. 11

Figure 1.7. Scanning electron microscopy images (SEM) of patterned polymeric structures formed using MIMIC. 12

Figure 1.8. Photograph and schematic drawing of the micro-transfer molding apparatus. 13

Figure 2.1. General scheme of the fabrication and functionalization of the maleimide containing 3D hydrogel patterns. 15

Figure 3.1. Photo-polymerization of FuMa-MA containing hydrogels and activation of FuMa-MA in the hydrogel structure by retro-DA reaction . 16

Figure 3.2. ^{1}H NMR results of unreacted reactant from bulk hydrogel. 18

Figure 3.3. TGA curves obtained from bulk-hydrogels; BH-0, BH-10, BH-0 and

BH-60 in nitrogen. 19

Figure 3.4. Swelling behavior of photopolymerized bulk-hydrogels; BH-0, BH-10, BH-30 and BH-60. 21

Figure 3.5. Swelling behavior of photopolymerized bulk-hydrogels BH-30-1. 21

Figure 3.6. SEM images of hydrogels; (a) BH-0 (b) BH-10 (c) BH-30 and (d) BH-60. …..... 22

Figure 3.7. SEM images of photopolymerized bulk-hydrogels BH-30-1. ..…….. 22

Figure 3.8. (a) UV-vis spectra of calibration curve for HABA/Avidin assay, (b) UV-vis spectra of the HABA/Avidin complex with biotinylated bulk-hydrogels. ……. 24

Figure 3.9. Schematic of micropatterning process (a) and characterization of patterned hydrogel microstructures; optical microscope image (b) and scanning electron microscopy images (c, d); scale bar is 10 μm (d). 26

Figure 3.10. Immobilization of BODIPY-SH on the hydrogel patterns and fluorescence microscope images of BODIPY-SH conjugated hydrogel pattern; HP-10 before (a) and after (b) retro-DA reaction. 27

Figure 3.11. Schematic of biotinylization and enzyme immobilization of hydrogel pattern. 28

Figure 3.12. Fluorescence microscope images and intensity profiles of FITC-streptavidin bounden biotinylated hydrogel patterns. 29

Figure 3.13. Fluorescence intensity profiles of BH-0 (a), BH-10 (b), BH-30 (c) and BH-60 (d). 30

LIST OF TABLES

Table 3.1. Photopolymerization of Bulk-Hydrogel in the presence of FuMa-MA. Photopolymerization condition. 17

Table 3.2. CHNS elemental analysis results of photopolymerized bulk-hydrogel, BH-0, BH-10, BH-30 and BH-60. 20

Table 3.3. Results of HABA/Avidin assay for bulk-hydrogel. 25

LIST OF ACRONYMS/ABBREVIATIONS

AIBN	2,2’-azobisisobutyronitrile
ATRP	Atom Transfer Radical Polymerization
$CDCl_3$	Deuterated chloroform
CH_2Cl_2	Dichloromethane
DA	Diels-Alder
DMPAP	4-Dimethylaminopyridine
EtOAc	Ethyl Acetate
FITC	Fluorescein isothiocynate
FT-IR	Fourier Transform Infrared
GPC	Gel Permeation Chromatography
MeOH	Methanol
NMR	Nuclear Magnetic Resonance
PEG	Poly(ethylene glycol)
PEGMEMA	Poly(ethylene glycol) methyl ether methacrylate
PMDETA	N,N,N-pentamethyldiethylenetriamine
rDA	Retro Diels-Alder
SEM	Scanning Electron Microscope
TEA	Triethylamine
TGA	Thermogravimetric Analysis
THF	Tetrahydrofuran

1. INTRODUCTION

1.1. Hydrogels

In recent years, enormous attention in biomedical sciences had been paid towards the fabrication of biocompatible hydrogels, biological polymers, and three-dimensional (3D) biomaterials [1]. Hydrogels are crosslinked hydrophilic polymer networks which can absorb from 10% up to thousands of times their dry weight in water. Hydrogels may be chemically stable or they may degrade and eventually disintegrate. Among the precursor polymers for synthesizing hydrogels are natural polymers such as collagen, chitosan and hyaluronic acid as well as biocompatible synthetic polymers such as poly(hydroxyethyl methacrylate), poly(ethylene glycol) and poly(vinyl alcohol). Therefore, they are of use in various biomedical applications such as biomolecular immobilization, tissue engineering, and fabrication of biosensors, artificial implants linings, and drug delivery [2].

Hydrogels can be synthesized either via physical interactions or chemical cross-linking. When the networks are constructed by molecular entanglements or secondary forces such as ionic, H-bonding or hydrophobic forces they are called ‘physical’ gels [3]. Li et al. showed synthesized a novel supramolecular hydrogel system which is a kind of physical hydrogel [4]. They used α-cyclodextrin and biodegradable poly(ethylene oxide)−poly[(R)-3-hydroxybutyrate]−poly(ethylene oxide) (PEO-PHB-PEO) triblock copolymer. It is very well known that poly ethylene oxide penetrates though α-cyclodextrin to form inclusion complexes via supramolecular interactions [5]. The complexation of PEO segments with α-cyclodextrin and the hydrophobic interaction between PHB blocks results in the formation of the supramolecular hydrogel (Figure 1.1).

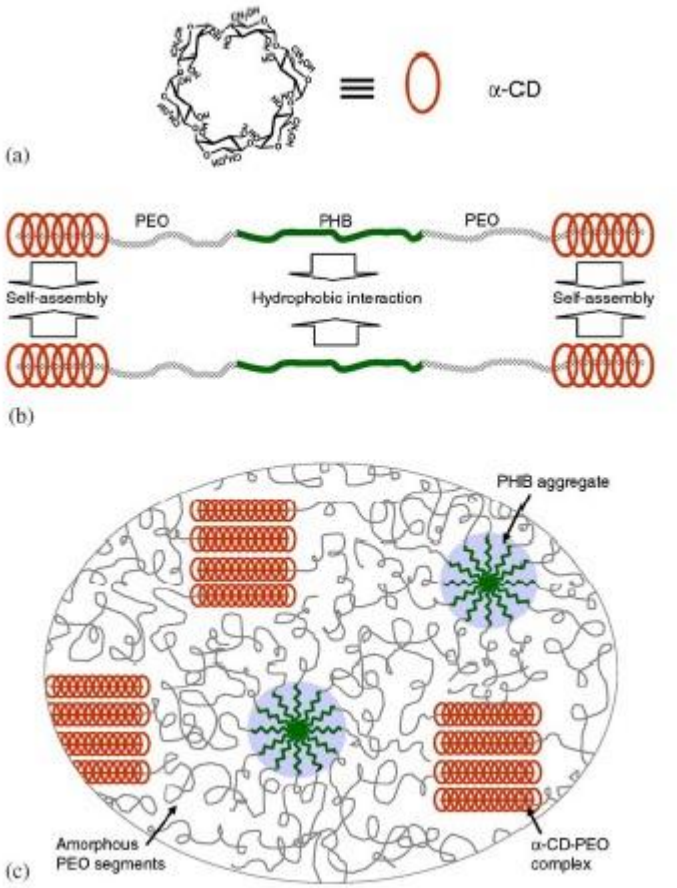

Figure 1.1. Physically crosslinked hydrogel.

However, it must be noted that physical hydrogels are not homogeneous, since clusters of physical interaction domains are present. Furthermore, the physical interactions may not be strong enough to provide stable and robust gels [6]. In order to construct stable networks, chemical cross linking of polymers is achieved via covalent bond formation. They generally form stable, non-reversible and robust hydrogels.

Examples for chemically cross linked hydrogel networks with the most commonly used mechanisms can be given as; azide functionalized PVA's clicked with alkyne appended PVA's [7], polymerization of peptides with ATRP [8], crosslinking with Diels-Alder reaction between PEG-bismaleimide and furan containing polymers [9], PEG-tetrathiols clicked with bisacrylates [10] to give hydrogel networks and photo cross-linking of acrylates in the presence of a photo initiator [11]. Indeed, by changing the type of the

polymer or reaction method or reaction conditions, we can tune the properties of hydrogels such as their swelling ability, cross link density, biodegradability, biocompatibility and functionality.

1.1.1. Functionalizable Hydrogels

Functionalization of hydrogel is achieved via covalent or non-covalent attachment. For applications like bio-immobilization, controlled drug delivery and protein delivery for tissue engineering, covalent attachment techniques are preferred to ensure control over attachment. Hydrogels can be utilized in such applications due to their capability of encapsulating various biomolecules in the interior matrix. They can exhibit controlled interactions between cells and proteins and slow release of drug molecules from the hydrogel matrix becomes possible in tissue engineering scaffolds.

The use of hydrogels as scaffolds for various applications derives from their ability to encapsulate various guest molecules in their interior. These guest molecules can be small molecules such as peptides or drug molecules that can be slowly released into the vicinity of an implant under physiological conditions [12] or growth factors or signaling peptide molecules for cell culture and tissue engineering applications [13]. Traditional approaches for incorporating entities into hydrogel matrix have relied upon encapsulation and physiabsorption. However, physiabsorption is limited due to the lack of control over rate and uniformity; in addition, it is not applicable to incorporation of cell adhesion peptides. For this reason, hydrogels bearing immobilized biomolecules have a great potential of use in tissue engineering.

To covalently immobilize biomolecules on hydrogels usually a monomer of the desired biomolecule is synthesized. For example West et al. synthesized a photo-chemically crosslinked hydrogel scaffold with covalently immobilized gradients of basic fibroblast growth factor (bFGF) using PEG-diacrylate and acryloyl-PEG-RGDS. It was observed that cells seeded on this hydrogel were aligned in the direction of increasing bFGF concentration within 24 hours [14]. In a later study, West and coworkers synthesized hydrogels containing covalently attached biotin and the cell adhesive peptide RGDS. They

utilized a PEG monomer which contains an activated ester at one terminus that allows attachment of any molecule of interest using the amidation chemistry, while the acrylate group at the other end allows covalent integration into the hydrogel and created 3D patterns using single photon absorbance (SPA) photolithography [15].

Hydrogels that contain molecules of interest integrated into the material through covalent attachment usually utilizes employment of a functional acrylate containing comonomer during the hydrogel synthesis. Hetero-bifunctional PEG such as acryloyl-PEG-NHS polymer has been widely utilized. This polymer contains an activated ester at one terminus that allows attachment of any molecule of interest using the amidation chemistry, while the acrylate group at the other end allows covalent integration into the hydrogel. In most cases, the macromonomer containing the *N*-hydroxysuccinimide-based activated ester is functionalized with the peptide fragment of interest prior to gelation. Hydrogels containing covalently attached biotin and the cell adhesive peptide RGDS have been fabricated using this approach.

However, covalent immobilization techniques have been generally limited to attachment of the molecule of interest into a polymerizable macromonomer [16]. Post-functionalization of hydrogels has been evaluated as an attractive alternative in recent years [17]. This approach relies on the presence of reactive functional groups in the hydrogel matrix that can undergo efficient functionalization under mild reaction conditions. Advent of “click” reactions [18] has dramatically influenced post-polymerization functional group transformations due to their near-quantitative conversions under mild reaction conditions. Indeed, recent works from Hilborn [19] and Hawker [20] groups have reported efficient synthesis of hydrogels using Huisgen type cross-linking of telechelic PEGs with multivalent azide based cross-linkers. Since then, many other groups have reported synthesis of hydrogels using the Huisgen click cycloaddition-based strategy [21].

Our research group showed synthesis of ‘clickable’ hydrogels utilizing the Huisgen-type copper-catalyzed click reaction between biodegradable polyester dendrons and biocompatible hydrophilic linear PEG polymers to access dendron−polymer−dendron conjugates necessary for the hydrogel formation [22]. In this study, functionalization of the

dendron periphery with alkyne groups affords reactive hydrogel precursors. While some alkyne groups are cross-linked via bis-azide to fabricate the hydrogel (second Huisgen type "click" reaction), the residual alkynes allow efficient covalent functionalization of the hydrogel matrix with molecules of interest via the third consecutive "click" reaction (Figure 1.2).

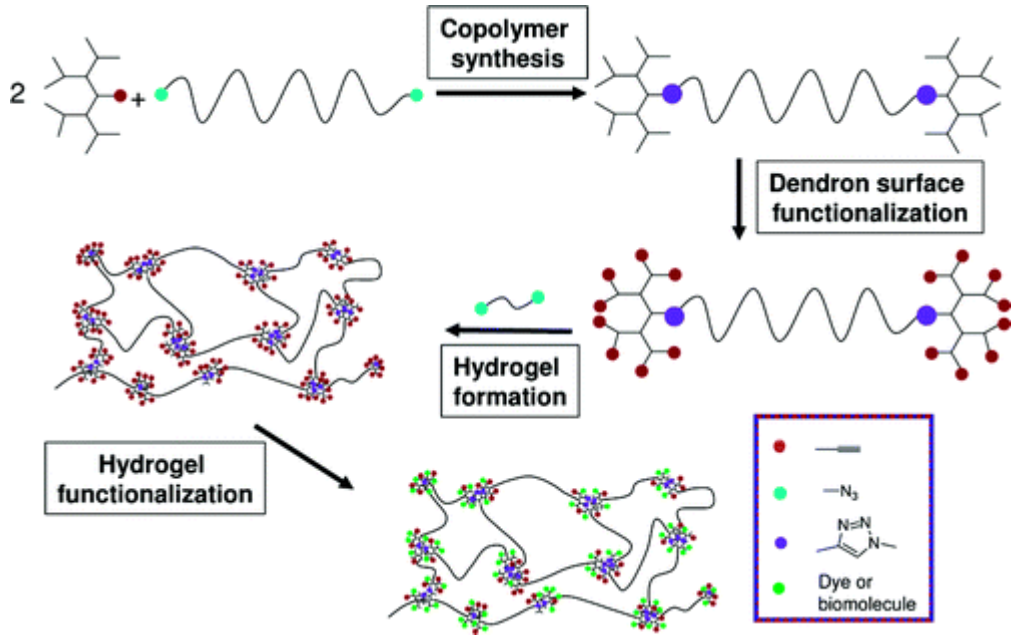

Figure 1.2. Hydrogel synthesized via click reaction from dendron-polymer-dendron conjugates.

For immobilization of biomolecules, a much sought after functionalization is via thiols since many biomolecules either contain or can be incorporated with cysteine residues at specific sites. Sulfhydryl group of the cysteine residues in biomolecules undergo facile reactions with maleimides [23], ortho pyridyl disulfide units [24], and vinyl sulfones [25]. The aforementioned functional groups have been incorporated in various polymers to provide a handle for conjugation of biomolecules to polymers to obtain polymer−biomolecule conjugates. Although the maleimide group has been extensively exploited in biomolecular immobilization using monolayers on various metallic and glass surfaces [26], examples of polymeric materials with maleimide side chains have been very limited. The limitation stems from the tendency of the reactive double bond of maleimide to participate in radical polymerization. Recently, remarkable advances have been made in

this area by utilization of protected maleimide-based initiators and monomers to obtain polymers with maleimide as their end groups and as side chains using a Diels−Alder reaction-based maleimide protection−deprotection strategy [27].

Especially, maleimide containing macromolecules are very advantageous used in biomolecular immobilizations due to its latent reactive character [28]. With Diels-Alder protection of this unit, active double bond does not participate to the polymerization or gelation process but lately can be activated for further conjugations. Recently, our group showed the fabrication of maleimide containing anti-biofouling hydrogels and these hydrogels are amenable to site-specific thiol conjugations [29]. In this work, novel hydrogels were synthesized via copolymerizing a furan protected maleimide based methacrylate monomer with PEGMA. Some of the maleimides undergo retro Diels-Alder reaction and acts as a crosslinker and free radical polymerization reaction ends up with gelation. After that, remaining free maleimides were activated and functionalized with thiol containing dyes and enzymes. Effects of temperature and feed ratio on the formation of these gels were investigated. (Figure 1.3).

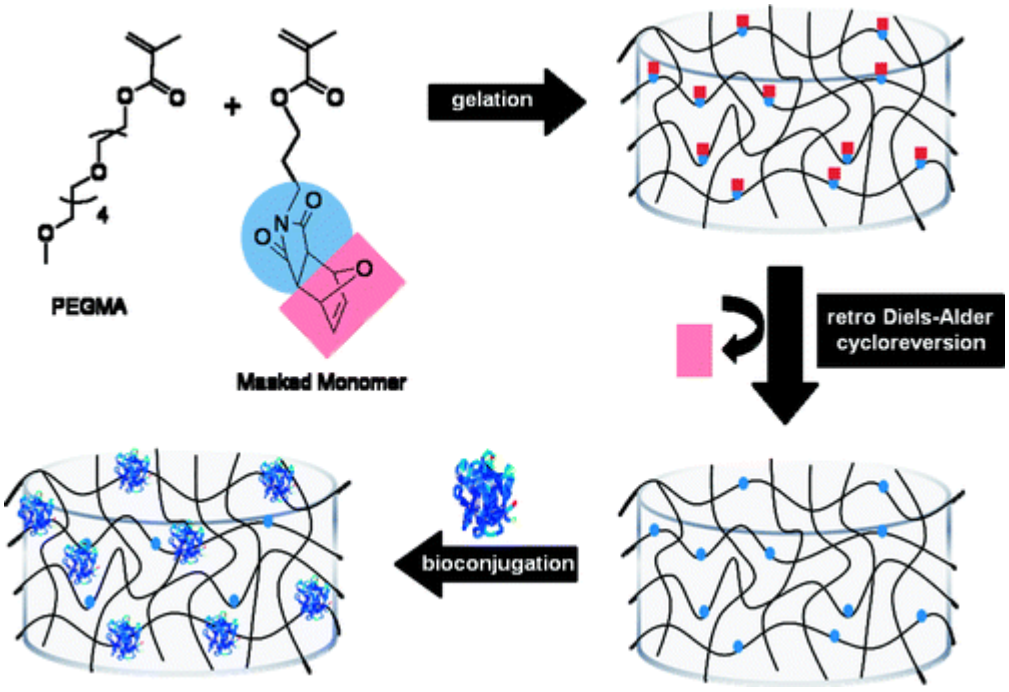

Figure 1.3. Thiol reactive hydrogels [29].

1.2. Soft Lithography and Microfabrication

Soft lithography based methodologies provides an easy access to micro and nanofabrication [30]. The term ‘soft lithography’ refers to a family of techniques for creating microstructures and nanostructures based on printing, molding and embossing [31]. The reason it is called "soft" that it uses elastomeric materials such as polydimethylsiloxane (PDMS). Soft lithography is generally used to construct features measured on the micrometer to nanometer scale.

All of the techniques in soft lithography utilize a layer of poly(dimethylsiloxane)(PDMS) or some other polymers with similar characteristics. The layer of PDMS is fabricated from a master by embossing, and typically has features with lateral dimensions of 1–1000 μm and vertical dimensions from 100 nm to hundreds of microns. The master is generally produced using photolithography [32] (Figure 1.4).

Pattern of master is obtained using computer-aided design. Patterns that have features with lateral dimensions are bigger than 10 μm are printed on a transparency via a printer [33]; and it is used as a mask for photolithography. For designs with features that have lateral dimensions smaller than 10 μm, the pattern is transferred to a thin layer of chrome on a glass slide using a laser or an electron-beam writer. A photoresist is coated on a silicon wafer or glass slide and the mask is placed between a source of ultraviolet light and a thin layer of a photoresist. Exposure to UV light transfers the pattern from the mask to the photoresist and the unexposed photoresist is washed away using organic solvent, leaving behind the three dimensional polymeric structure. A silicon wafer with polymeric photoresist structures patterned on its surface is referred to as the master [32].

To make PDMS masters, the liquid prepolymer of PDMS is mixed and poured on the surface of the master. After curing thermally (at 65°C), the layer of PDMS is peeled away and contains the inverse of the original pattern. The prepolymer of PDMS is commercially available and inexpensive. It is prepared by mixing two the base polymer with a curing agent basically.

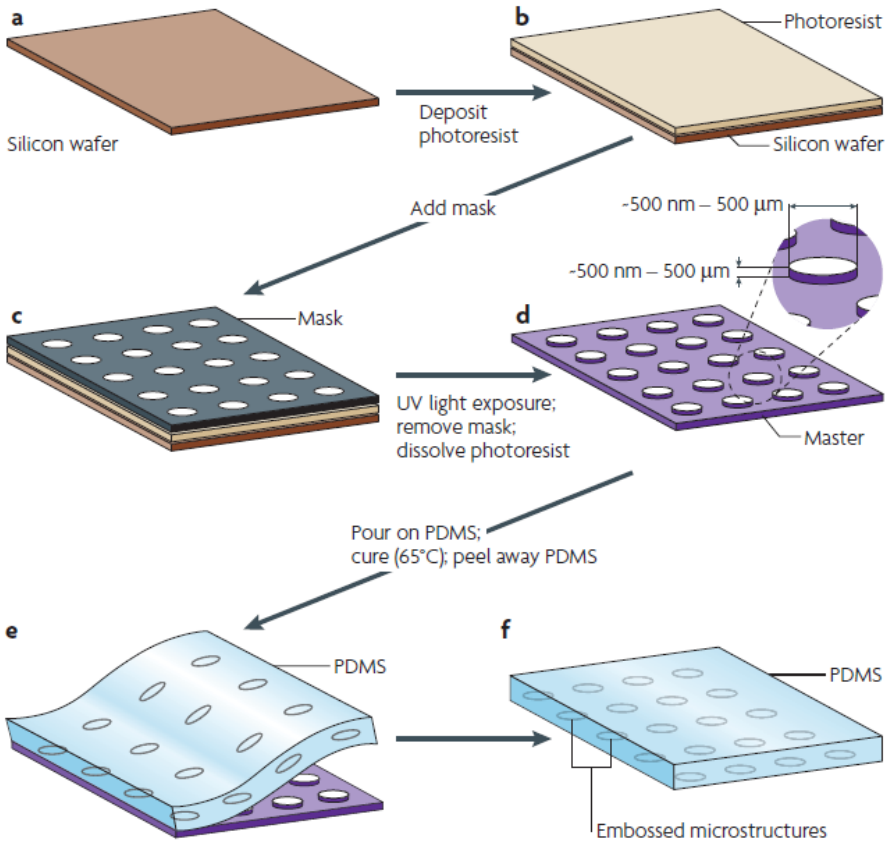

Figure 1.4. The fabrication of micropatterned slabs of PDMS [32].

1.2.1. The Tools of Soft Lithography

1.2.1.1. Replica Molding (REM). In replica molding method, a pre-polymer in the liquid state is cast on the master structure and polymerised in situ, generally by thermal curing. The elastomeric replica can then be peeled-off from the master. The REM process can also be iterated, for instance it is possible to realise a first replica by PDMS from the master, and then a second replica by a different curable polymer, but this time using the first replica as mold. A patterned layer of PDMS functions as the mold in this technique and is used to transfer the pattern to the surface of another polymer. A prepolymer is deposited on the PDMS mold, is cured, and then separated from the master by peeling them apart (Figure 1.5). This technique has been used to micropattern biocompatible polymers. The costs for REM and the subsequent soft lithographic steps are quite low which makes these techniques accessible to many laboratories [34].

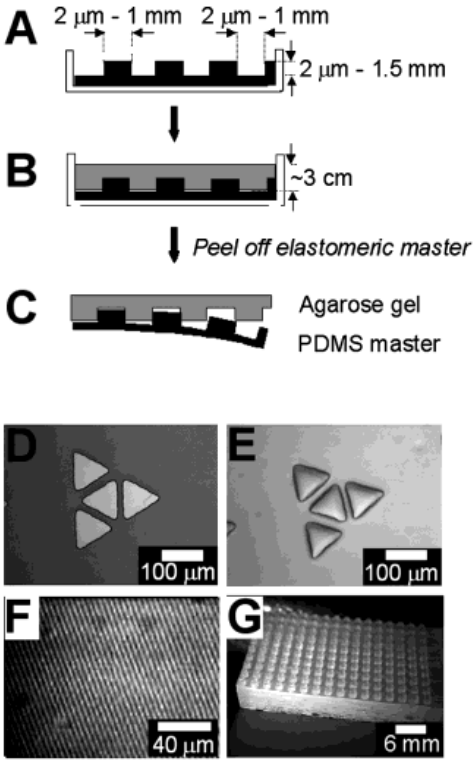

Figure 1.5**.** Fabrication of micropatterned agarose gels via replica molding [35].

1.2.1.2. Microcontact Printing. Microcontact printing (μCP) is one of the most common soft lithography methods because it is easy to perform and can be used for many applications. Microcontact printing locally transfers ink molecules from the surface of a patterned PDMS stamp to the surface of a substrate upon physical contact.

In the first studies, micro contact printing was used to print monolayers of alkyl thiols on gold surfaces [36]. The sulfur atom of the ink chemisorbs to the gold surface and a dense self-assembled monolayer (SAM) is formed within seconds. However, μCP is not limited to printing thiols on gold surfaces only. Various materials, including small biomolecules, proteins, polyelectrolytes and suspensions of cells, can be patterned directly on surfaces using microcontact printing. It has been shown in literature that silanes [37], lipids [38], proteins [39], DNA [40], synthetic polymers [41] and nanoparticles [42] can be printed by μCP.

In this technique, contact between the PDMS stamp and a substrate only transfers ink molecules from the patterned surface of the base relief features of the stamp to the substrate, and generates patterns with very small feature sizes like 100 nm over large areas like 1 m^2. The elasticity of the PDMS stamp facilitates conformal contact between the stamp and the substrate, and makes patterning on non-planar surfaces such as porous, rough or curved surfaces possible.

Ravoo and Reindhoudt showed that microcontact printing is also an advantageous tool for catalysts free Huisgen 1,3-dipolar cycloaddition reaction [43]. In this work they generated azide terminated monolayer on Si/ SiO_2 surface. Using alkyne terminated dye molecule (LRA) they fabricated dye patterns via micro contact printing technique and visualize these patterns via fluorescence microscope. With control experiment using (monolayer on Si/SiO_2 without azide group) and they proved that Huisgen click reaction works via micro contact printing without copper catalysts which is toxic for bio-applications (Figure 1.6).

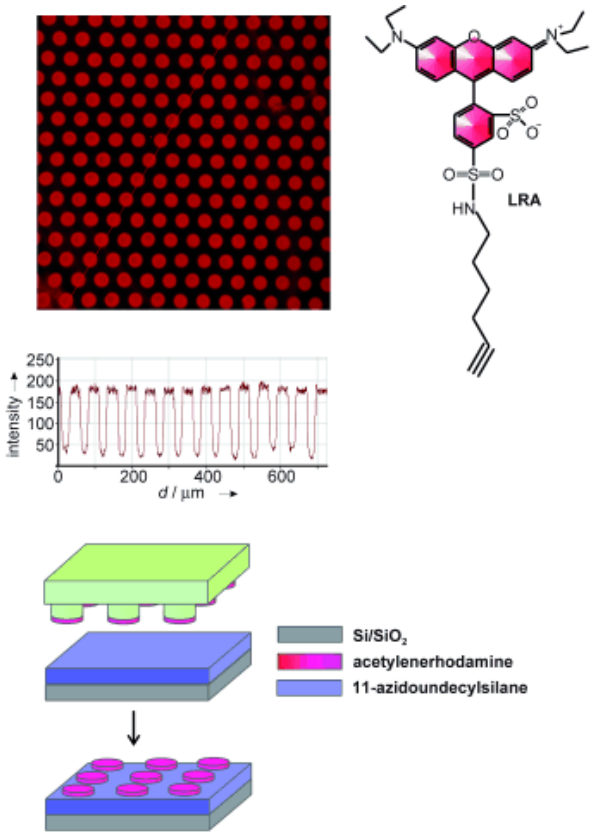

Figure 1.6. Catalysts free Huisgen 1,3-dipolar cycloaddition reaction via micro contact printing technique [43].

1.2.1.3. Micromolding in Capillaries (MIMIC). A recent promising soft lithographic method is Soft Molding (SM) in other words capillary force lithography (Figure 1.7) [44]. This technique combines soft and nanoimprint lithography using elastomeric elements and exploiting the glass transition of organic compounds to transfer the pattern. In this method the mold is placed onto a polymeric film, which is driven above the glass-transition temperature (T_g) of the target compound. After cooling-down the subsequent below T_g freezes the pattern into the polymer, the replica can be then peeled-off. The soft moulding is based on the capillarity effect forcing the polymer to penetrate into channels of the elastomeric stamp.

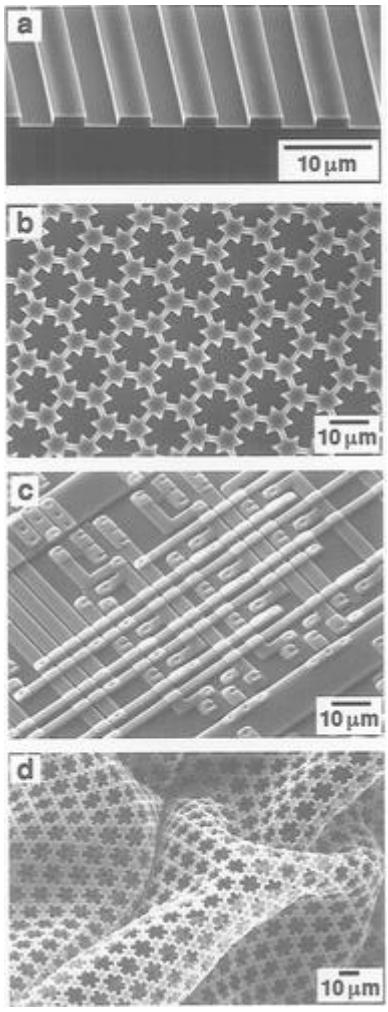

Figure 1.7. Scanning electron microscopy images (SEM) of patterned polymeric structures formed using MIMIC. (a), (b) and (c) are polyurethane patterns, (d) free-standing film formed using the structure in (b), after removal the film from its support [44].

MIMIC is a complementary technique to nano imprinting lithography (NIL) and has several advantages over the NIL process. In fact, since the penetration of the polymer into

the features of the mold is driven by capillarity effects, SM is marginally affected by problems of difficult polymer transport, as compared to the high pressures conditions under which NIL is carried out. More importantly, the SM technique is cheaper because it does not need any press set-up to ensure the contact between the mold and the polymer. This is because in most cases the soft elastomeric material strongly adheres to the surface.

1.2.1.4. Microtransfer Moulding. Microtransfer moulding is a technique for patterning polymeric materials in which a thin layer of a liquid prepolymer is applied to the patterned surface of a PDMS stamp [32]. In this method, firstly features of the stamp filled with prepolymer. Then it is brought into conformal contact with a surface, and the prepolymer is cured. When the stamp is peeled away, patterned microstructures remain on the surface of the substrate. This technique is simple and does not need any expensive equipments and it produces three-dimensional structures with feature sizes as small as ~1 μm in a single step (Figure 1.8).

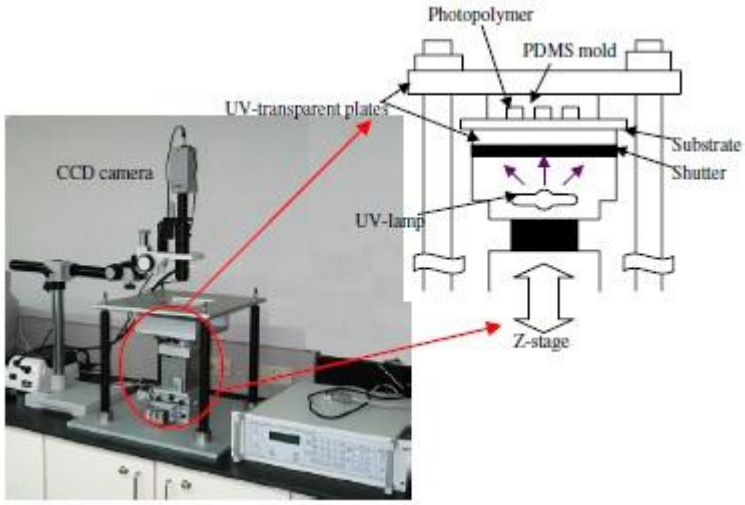

Figure 1.8. Photograph and schematic drawing of the micro-transfer molding apparatus [45].

1.3. Patterned Hydrogels

Patterned hydrogels are often designed to mimic natural tissue and are mainly used in tissue engineering [46]. Current methods of patterning hydrogels include photoreaction injection [47], photolithography [48], microfluidic patterning [49], microcontact printing [50] and electrochemical deposition [51]. Photo-polymerization or photo-crosslinking method has been used for obtaining patterned of hydrogel due to its several advantages over conventional polymerization methods; spatial and temporal control over polymerization, fast curing rates at room temperature under physiological conditions. There are several biomedical applications of photopolymerized hydrogel, for example, prevention of thrombosis [52], post-operative adhesion formation [53], drug delivery [54], coatings for biosensors [55] and for cell transplantation [56]. Many different methods have been used extensively for 3D structured polymer patterns, including, replica molding [57], capillary force lithography [58] and micromolding in capillaries [59]. Recently, Spring *et al.* has reported PEG based hydroxysuccinimide (NHS) 3D hydrogel pattern in presence of PEG-diacrylate cross-linker and photoinitiator for small-molecule microarraying purposes by micro contact printing technique and studied bioimmobilization. The 3D hydrogel pattern display improved loading capacity, signal sensitivity and spot morphology compared with 2D patterns [60].

2. AIM OF THE STUDY

Aim of this study is fabrication of novel thiol reactive hydrogels. Bulk and patterned hydrogel can be prepared by photo-polymerization in presence of PEG-DA cross-linker and a masked maleimide-based methacrylate monomer (FuMa-MA). The masked-maleimide groups in the hydrogels can be deprotected by retro Diels-Alder (rDA) reaction to render them reactive toward thiol containing molecules by Michael addition conjugation reaction. Incorporation of tailored amount of the thiol-reactive monomer into the feed, allows fabrication of hydrogels with control over extent of functionalization. Extent of incorporation the thiol reactive maleimide groups and their availability for conjugation with thiol containing molecules can be determined by attachment of fluorescent dye and immobilization of FITC-streptavidin on the biotinylated hydrogels.

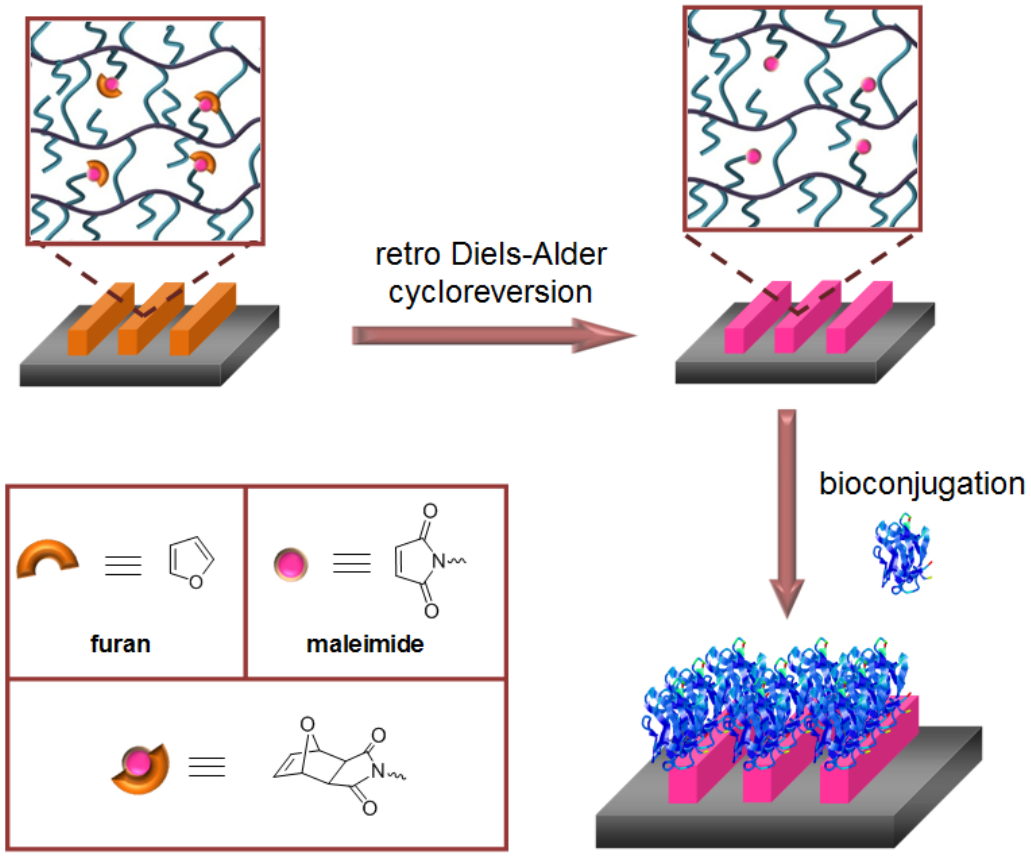

Figure 2.1. General scheme of the fabrication and functionalization of the maleimide containing 3D hydrogel patterns.

3. RESULTS AND DISCUSSION

3.1. Synthesis of Photopolymerized Bulk-Hydrogel

The cross-linked hydrogel by photo-polymerization in presence of PEG-DA as a cross-linker was performed at various amount of FuMa-MA which is thiol-reactive after retro-DA reaction (Figure 3.1). The recipe and the reaction parameters investigated in this study are summarized in Table 3.1, where Bulk-hydrogels are symbolized by BH-X (X means the percent weight fraction of FuMA-MA in feed with respect to PEGMEMA and PEG-DA). The photo-polymerization of bulk-hydrogels were resulted in transparent gel with 97~98% conversion.

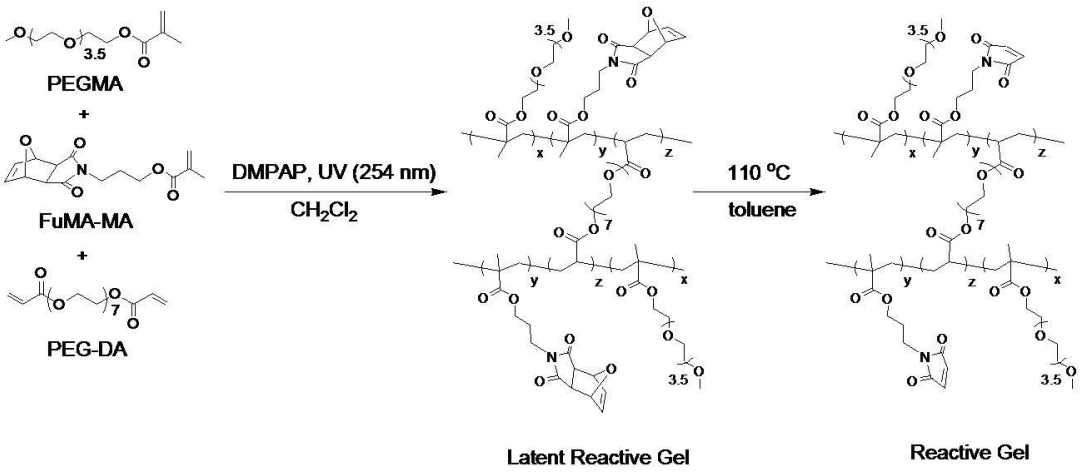

Figure 3.1. Photo-polymerization of FuMa-MA containing hydrogels and activation of FuMa-MA in the hydrogel structure by retro-DA reaction.

In order to understand FuMa-MA monomer conversion of photo-polymerization of bulk-hydrogel, unreacted reactants from gels (BH-10, BH-30 and BH-60) were analyzed by ^{1}H NMR (Figure 3.2) and FuMa-MA monomer conversion was obtained 98~99%. Photopolymerization of 30% FuMa-MA containing hydrogel was carried out in the water/methanol (1:1, v/v) solvent system prior to prepare hydrogel in DCM. The conversion of polymerization was obtained 94% in like manner to BH-0, BH-10, BH-30, and BH-60. These results show that there are not much difference between water/methanol solvent and dichloromethane for photopolymerization of hydrogel. Due to higher solubility

of FuMa-MA in organic solvent, this is not so surprising since hydrogel formation in our case does not involve any preorganization of the reactants in the solvent, unlike photo-crosslinked hydrogels obtained via crosslinking of ABA triblock copolymers. In this work we used dichloromethane as solvent for fabrication of bulk-hydrogels and preparation of hydrogel micro patterns.

Table 3.1. Photopolymerization of Bulk-Hydrogel in the presence of FuMa-MA. Photopolymerization condition; PEGMEMA = 200 mg, PEG-DA = 27 mg, DMPAP = 50 mg, DCM = 0.1 mL, UV (254 nm) illumination time = 40 min, room temperature. [a]bulk-hydrogel by photopolymerization without FuMa-MA. [b]calculated from the amount of furan released as observed in TGA. [c]conversion = (dry gel weight / total weight of monomer) × 100.

sample	FuMA-MA in feed (mg)	Furan(%) observed [b]	Furan(%) theoretical [b]	Conversion (%)[c]
BH-0 [a]	-	0	0	97
BH-10	22	1.97	2.065	98
BH-30	66	6.08	6.195	97
BH-60	132	10.95	12.390	99

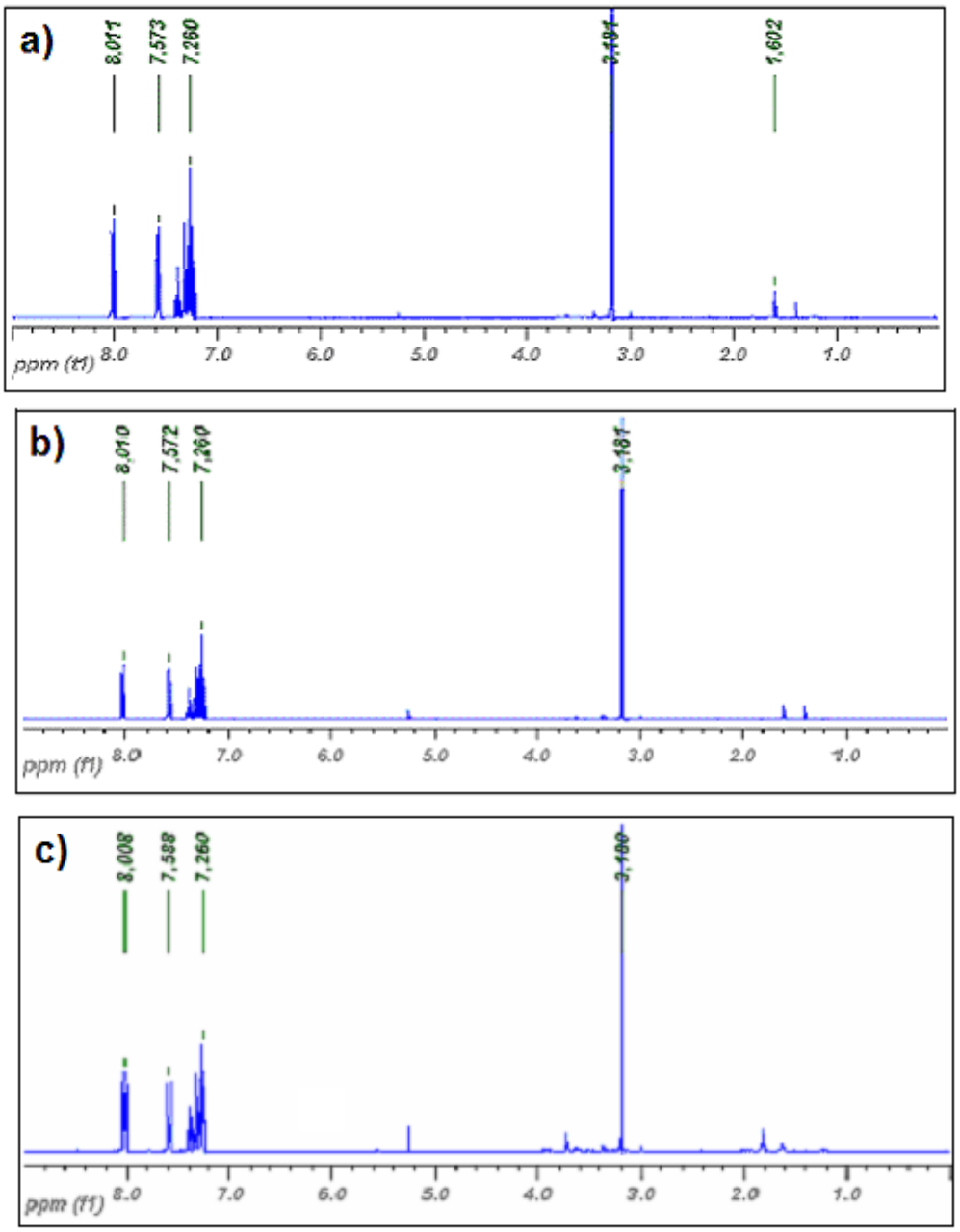

Figure 3.2. ^{1}H NMR results of unreacted reactant from bulk hydrogel.

3.2. Thermogravimetric Analysis of Hydrogels

TGA analysis of bulk-hydrogel was used to determine the amount of the FuMa-MA functional group in the gel. Bulk-hydrogel samples were analyzed before retro-DA reaction at 110°C. The TGA result of hydrogels contain FuMa-MA (BH-10, BH-30, BH-60) indicates a continuous weight loss starting from 60 to 180°C, associated with

decomposition of furan protected maleimide group of FuMa-MA by retro-DA reaction [61]. According to the TGA analysis the observed weight losses were 1.97%, 6.08% and 10.95% for bulk-hydrogel BH-10, BH-30 and BH-60, respectively. From TGA results, a consistent increase in weight loss of the bulk-hydrogel was observed upon increasing the amount of FuMa-MA and observed furan weight loss were close to the theoretical values.

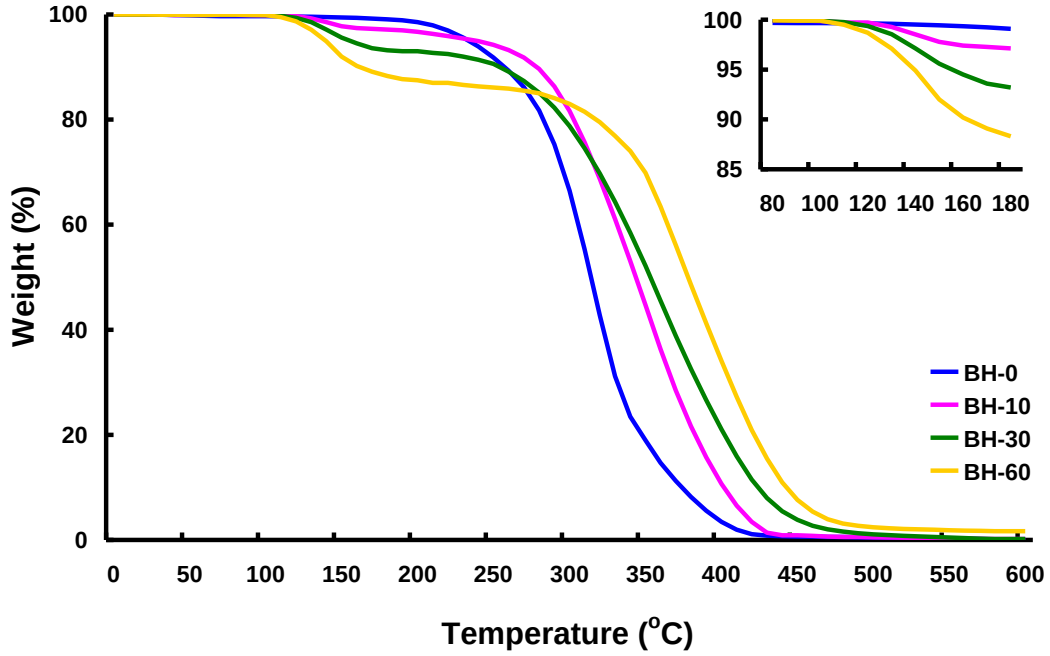

Figure 3.3. TGA curves obtained from bulk-hydrogels; BH-0, BH-10, BH-30 and BH-60 in nitrogen.

3.3. Elemental Analysis of Bulk-Hydrogels

In order to ascertain the FuMa-MA contents increasing in bulk-hydrogel, CHNS elemental analysis was accomplished. From the elemental analysis, significant increase in total N content in the gel was observed as the amount of fed FuMa-MA increased (Table 3.2).

Table 3.2. CHNS elemental analysis results of photopolymerized bulk-hydrogel, BH-0, BH-10, BH-30 and BH-60.

Sample	Theoretical Value			Obtained value		
	%C	%H	%N	%C	%H	%N
BH-0	57.81	6.10	0	56.10	7.44	0
BH-10	58.15	6.11	0.43	55	8.60	0.36
BH-30	58.68	6.12	1.10	55.79	8.46	0.85
BH-60	58.25	7.68	1.75	58	7.81	1.46

3.4. Swelling Study of Bulk-Hydrogel

Figure 3.4 depicts the swelling study results for the photopolymerized bulk-hydrogels, BH-0, BH-10, BH-30 and BH-60. As the concentration of the relatively hydrophobic FuMa-MA segments increased, the swelling rate as well as the extent of swelling of the hydrogels decreased. For example, the swelling ratio of the BH-0 hydrogel reached 146% after 30 h immersion; while, at the same period (30 h), the swelling ratios were 97, 49 and 29% for BH-10, BH-30, and BH-60 hydrogels, respectively. Additionally, swelling behavior of BH-30-1 was studied to compare with BH-30. Water uptake of BH-30-1 was obtained as 52% (Figure 3.5) and it shows that BH-30-1 has similar swelling property as BH-30 (49%).

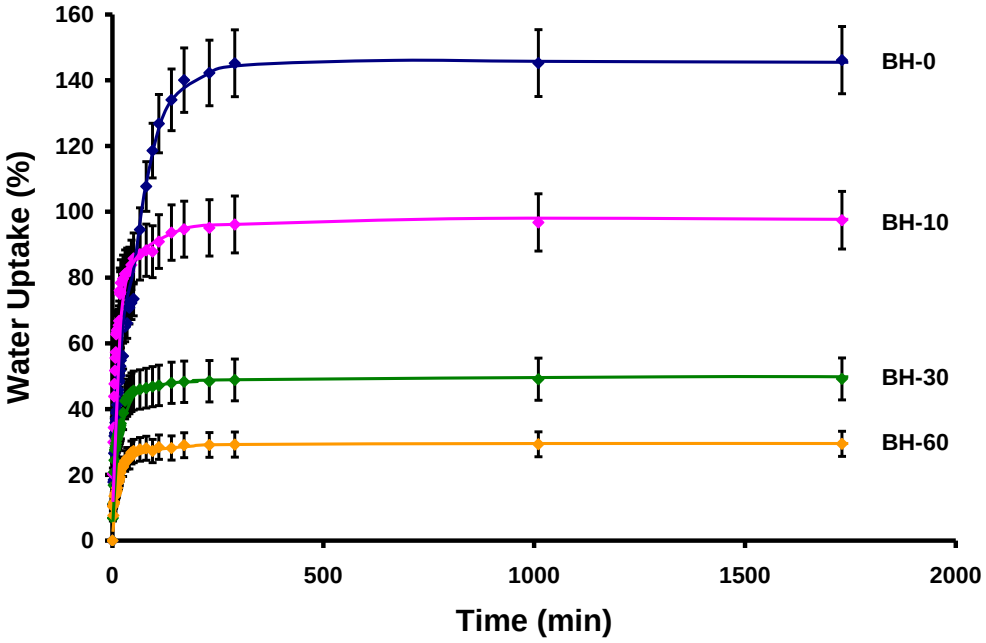

Figure 3.4. Swelling behavior of photopolymerized bulk-hydrogels; BH-0, BH-10, BH-30 and BH-60.

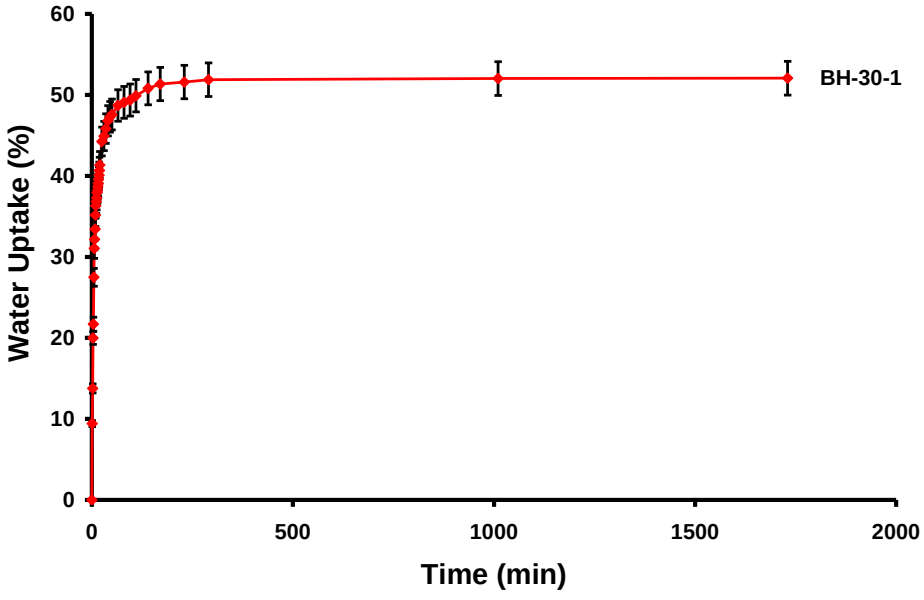

Figure 3.5. Swelling behavior of photopolymerized bulk-hydrogels BH-30-1.

3.5. Morphology Analysis of Bulk Hydrogels

Morphology of the bulk-hydrogels was investigated with SEM (Figure 3.6 and Figure 3.7). For all bulk-hydrogel samples have fewer pores in the structure and tight rubber like structure even aqueous solvents were used for photopolymerization of hydrogels. In this work, PEG-DA was used as a cross-linker to form hydrogel and it was covalently bounded to double bond of two monomers, PEGMEMA and FuMa-MA during photopolymerization. The obtained morphologies are similar to other literature examples, PEG-DA crosslinker had been used to make mechanically stable highly crosslinked hydrogels [62-64].

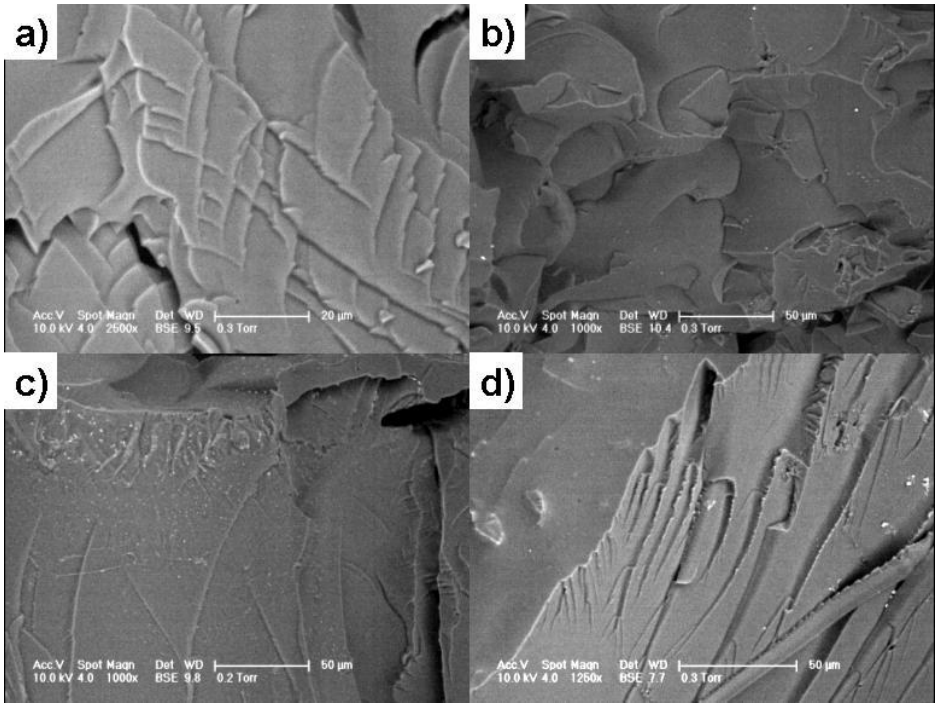

Figure 3.6. SEM images of hydrogels; (a) BH-0 (b) BH-10 (c) BH-30 and (d) BH-60.

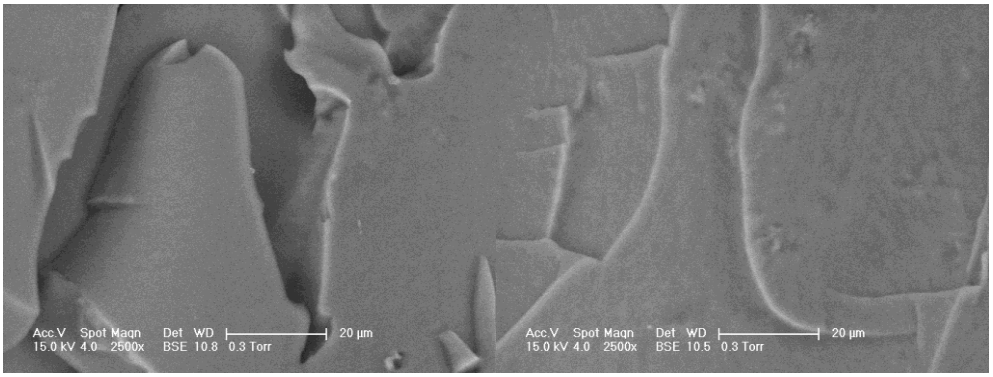

Figure 3.7. SEM images of photopolymerized bulk-hydrogels BH-30-1.

3.6. Biotin Concentration Determination

To estimate the availability of thiol-reactive maleimide in bulk-hydrogel, the amount of biotin attached on maleimide in bulk-hydrogel was quantified by HABA/Avidin assay [65]. Since biotin has a much higher affinity for the binding sites in avidin ($K_d \approx 10^{-15}$ M for avidin complex with free biotin), when present it stoichiometrically displaces HABA (dissociation constant $K_d \approx 10^{-6}$ M) from the avidin [66]. When HABA bounds to avidin, it exhibits a UV spectral absorbance at 500 nm. Since only the HABA/Avidin complex has absorption at 500nm, the amount of released HABA can be determined by UV Abs500 readings when sites become occupied by biotin. Figure 3.8 shows the UV-vis spectra of calibration absorbance of HABA/Avidin complex and the spectroscopic changes of the complex upon the addition of biotinylated bulk-hydrogel. UV-vis spectra of calibration curve for HABA/avidin assay shows a decrease in the absorbance of the complex as free biotin concentration changed from 0 to 9μM. (Figure 3.8a) On basis of the calibration curve (Figure 3.8b), the amount of available biotin in the biotinylated hydrogels were calculated (Table 3.3). As expected, higher numbers of biotins were detected in hydrogels containing more maleimide groups. BH-60, BH-30 and BH-10 were shown to possess 0.85, 0.49 and 0.18 $\mu mol.mg^{-1}$ of available biotin, respectively.

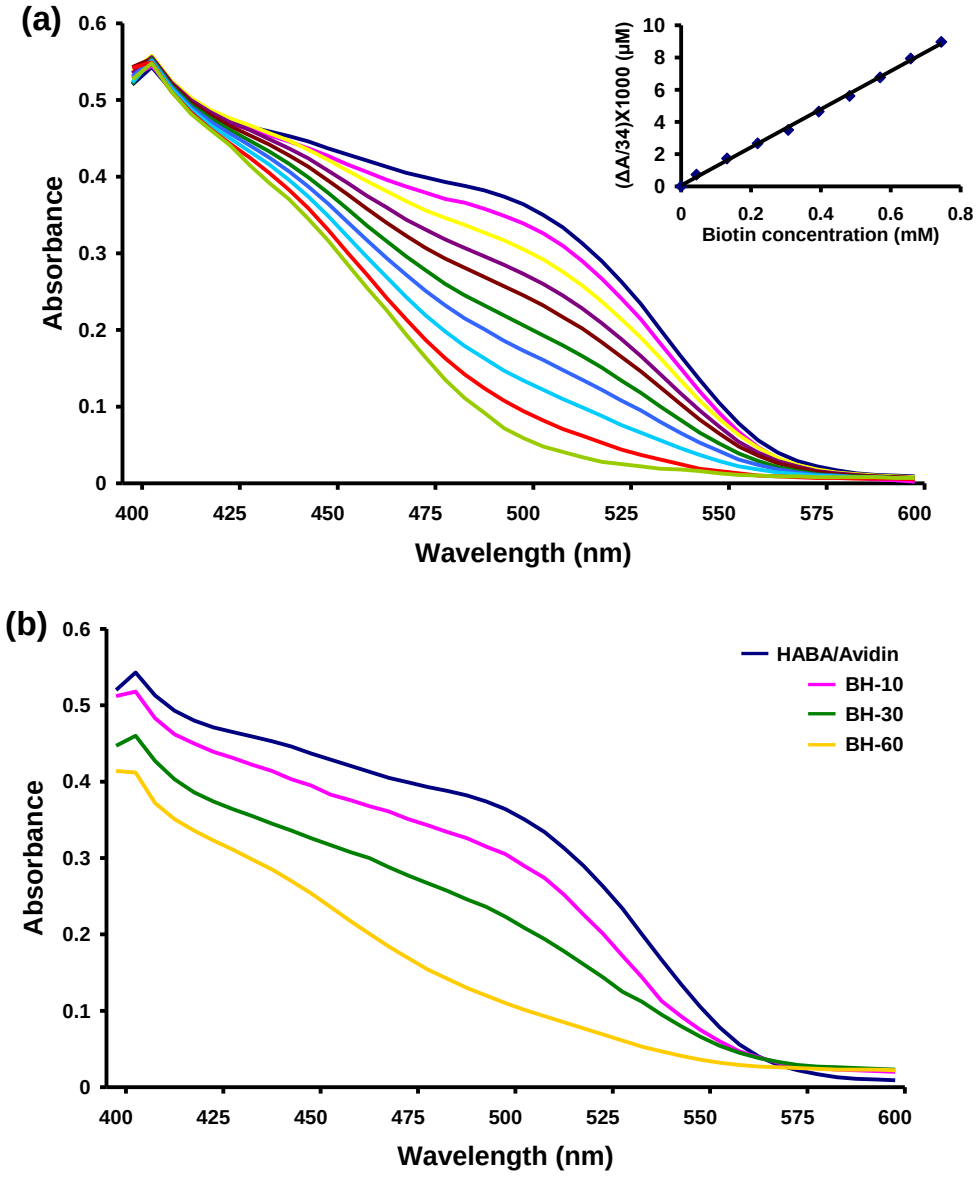

Figure 3.8. (a) UV-vis spectra of calibration curve for HABA/Avidin assay, and in set is the calibration curve of HABA/Avidin assay, (b) UV-vis spectra of the HABA/Avidin complex with biotinylated bulk-hydrogels, HP-10, HP-30 and HP-60.

Table 3.3. Results of HABA/Avidin assay for bulk-hydrogel. [a]Theoretical values of the surface-available biotins based on the initial molar ratios of the biotinylated hydrogels. [b]Available biotin in the hydrogel by comparison of the absorbance change with that of the calibration curve (Figure 5a). [c]Available biotin per gram of hydrogels based on the calculated concentration of the sample solutions used in each assay.

Sample	theoretical value of available biotin [a] ($\mu mol.mg^{-1}$)	available biotin per milliliter of sample solution [b] ($\mu mol.mL^{-1}$)	available biotin per gram of hydrogel [c] ($\mu mol.mg^{-1}$)
BH-10	0.29	0.17	0.18
BH-30	0.75	0.39	0.49
BH-60	1.25	1.22	0.85

3. 7. Preparation and Activation of Photopolymerized Hydrogel Pattern (HP)

The reaction scheme for the preparation and streptavidin immobilization of patterned hydrogel (HP) by photopolymerization is illustrated in Figure 3.9. In order to promote adhesion of hydrogels onto the silicon surface, interfacial bonding photopolymerization was utilized. For this purpose, 3-(trimethoxysilyl) propyl methacrylate (TMSPMA) with C=C groups was reacted with Si–OH groups on the surface of silicon wafer. Hydrogel patterns on the silicon wafer were prepared by capillary reaction with PDMS stamp. The optical microscope and SEM images of hydrogel pattern are shown in Figure 3.9. It was observed from microscope imaging that hydrogel patterns were successfully prepared by photopolymerization whose average width of pattern was 30μm (Figure 3.9b).The wrinkled edge of is made according to the shape of the original PDMS pattern (Figure 3.9c,d). The photopolymerized hydrogel patterns are symbolized by HP-X like a BH for bulk-hydrogel, X means the percent weight fraction of FuMa-MA in feed with respect to PEGMEMA and PEG-DA. The hydrogel patterns are heated at 110°C under the vacuum for 30 min in order to obtain deprotected FuMa-MA side group, furan protected maleimide, in the hydrogel structure by re-DA reaction. Deprotected maleimide can be functionalized with thiol containing biomolecules. These hydrogel patterns adhered well onto the silicon surfaces and did not peel off after prolonged immersion and washing with various solvents.

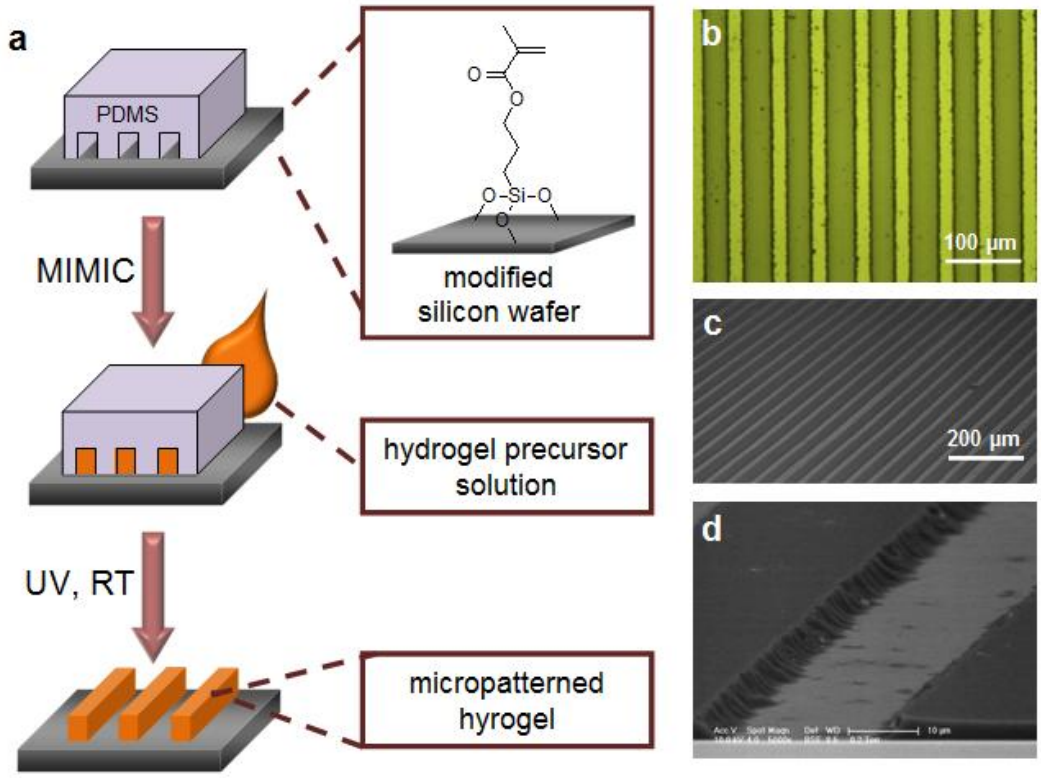

Figure 3.9. Schematic of micropatterning process (a) and characterization of patterned hydrogel microstructures; optical microscope image (b), and scanning electron microscopy images (c, d); scale bar is 10 µm (d).

3. 8. Dye Immobilization on Patterned Hydrogels

The efficiency of functionalization of these hydrogel patterns contain various amount of functionalizable maleimide, HP-0, HP-10, HP-30 and HP-60, was studied by conjugation of a thiol containing fluorescent dye BODIPY-SH prior to attach biomolecules to hydrogel patterns. As a control experiment, the latent reactive HP-10 hydrogel patterns were exposed to BODIPY-SH. Figure 7 shows the process of immobilization of BODIPY-SH in the hydrogel pattern and results of fluorescence microscope image after BODIPY-SH immobilization. As expected, hydrogel HP-10 prior to activation by retro-DA reaction has no fluorescence (Figure 6a). Activated HP-10 hydrogel pattern, on the other hand, was fluorescent due to presence of thiol reactive maleimide after activation by retro-DA reaction. BODIPY-SH immobilization was carried out onto activated HP-30 and HP-60 hydrogel patterns with same process as HP-10. But the fluorescence intensity of hydrogel

patterns was decreased as thiol reactive maleimide fraction is increased in the hydrogel pattern. These results are because of self-quenching of bodipy dyes. The self-quenching arises as a result of energy transfer among molecules of a fluorophore and is also referred to as quenching due to the formation of statistical traps. The type of fluorophore concentration dependence of quenching has been described that if two fluorophore molecules are at or within a critical distance, they are assumed to from a statistical pair that acts as an exciton trap [38, 39]. Immobilization of fluorescently labeled enzyme was attempted thereafter, since self-quenching process will be minimal due to larger separation of the dye molecules.

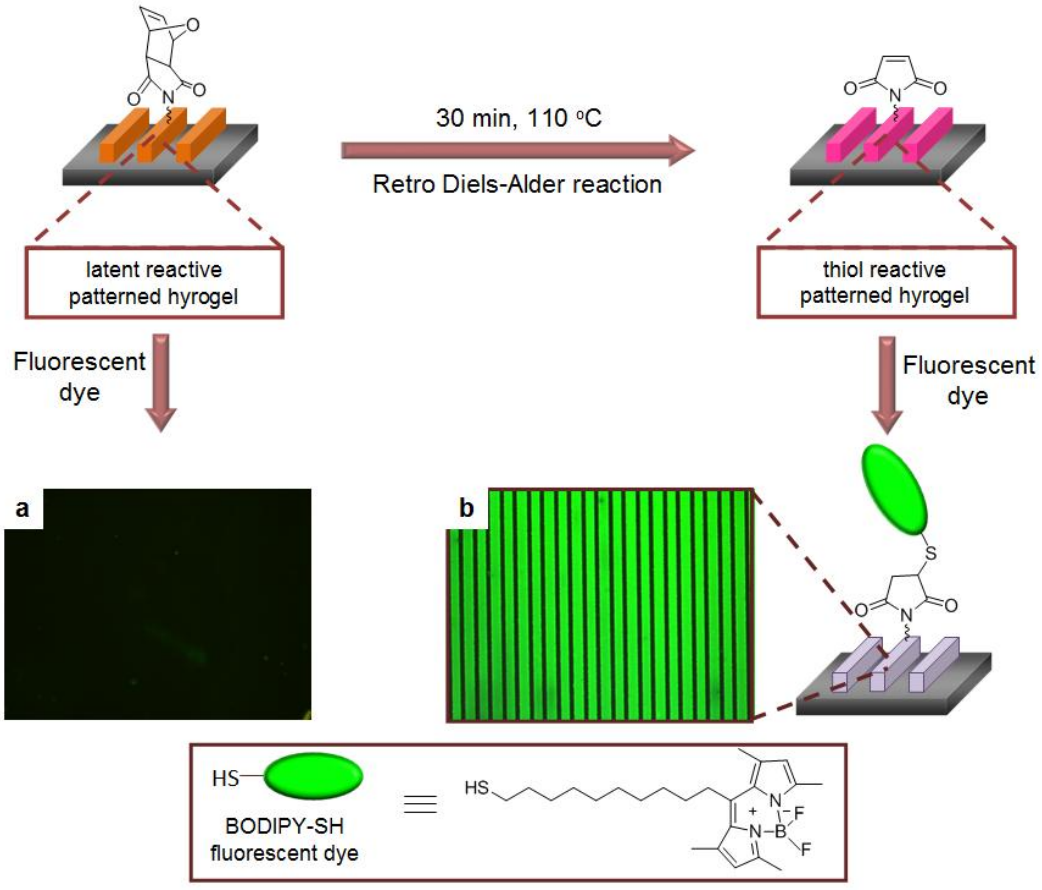

Figure 3.10. Immobilization of BODIPY-SH on the hydrogel patterns and fluorescence microscope images of BODIPY-SH conjugated hydrogel pattern; HP-10 before (a) and after (b) retro-DA reaction.

3.9. Streptavidin Immobilization on the Biotinylated HP

Biomolecular immobilization of a fluorescently labeled enzyme, namely FITC-streptavidin, was used to demonstrate increased extent of functionalization by increasing the reactive functional group in the hydrogel matrix. Conjugation of biotin-SH onto the patterned hydrogels with varying amount of maleimide made them amenable to specific immobilization of streptavidin (Figure 3.11).

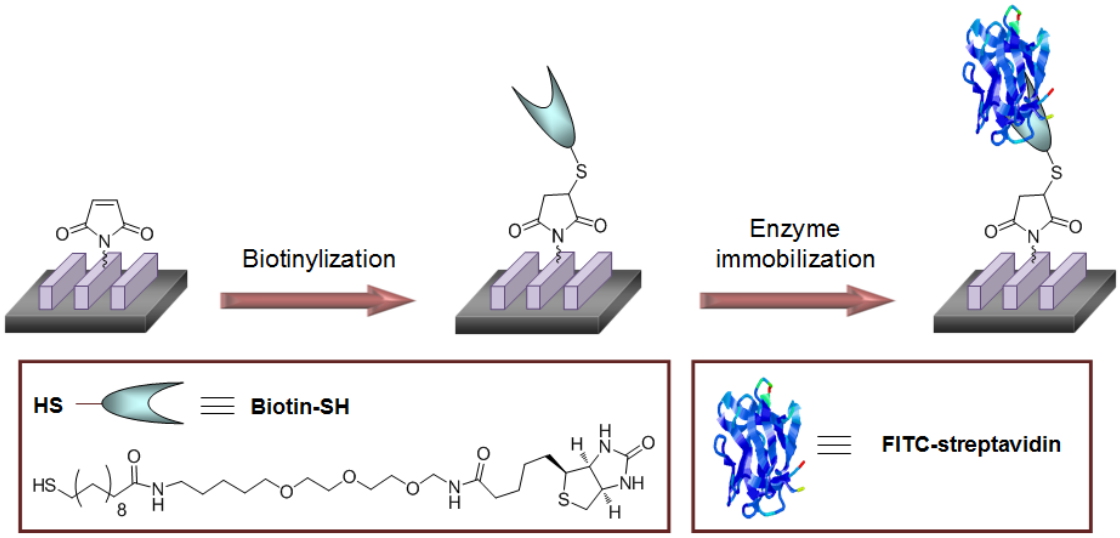

Figure 3.11. Schematic of biotinylization and enzyme immobilization of hydrogel pattern.

Biotin is a ligand known to bind onto streptavidin through strong specific noncovalent binding. All hydrogel patterns, HP-0, HP-10, HP-30 and HP-60, were reacted with excess thiol containing biotin which can react with activated maleimide. Patterns were exposed to FITC-streptavidin to visualize the efficiency of functionality due to various amount of maleimide in hydrogel patterns, after washing off excess biotin from the hydrogel patterns to remove any unbound ligands. After washing off physiabsorbed streptavidin from the hydrogel pattern, fluorescence microscope was performed to investigate the extent of immobilization.

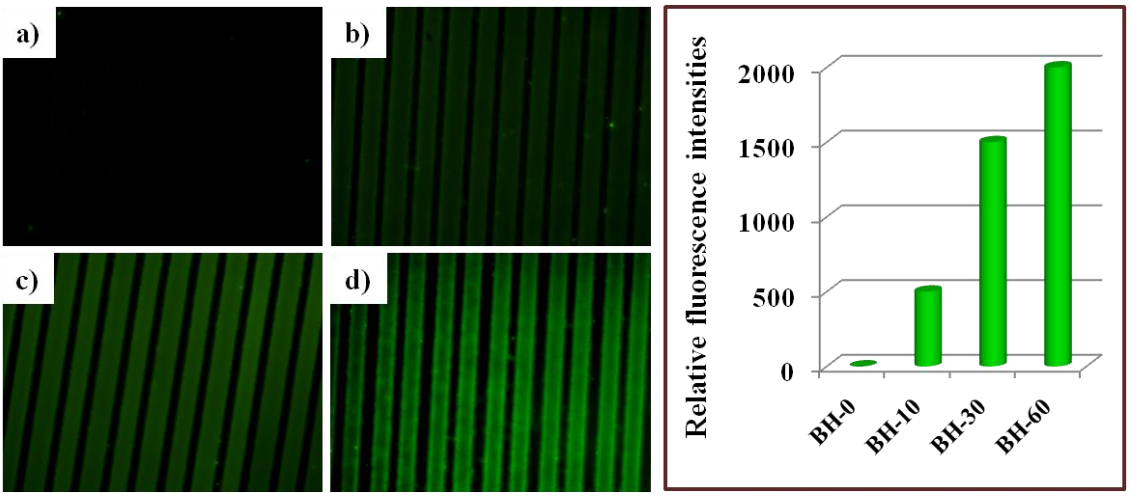

Figure 3.12. Fluorescence microscope images and intensity profiles of FITC-streptavidin bounded biotinylated hydrogel patterns; HP-0 contains no covalently bounded biotin ligand (a), HP-10 (b), HP-30 (c) and HP-60 (d).

The amounts of FITC-streptavidin in the gel is increasing according to increase of amount of covalently bound biotin ligands which is react with activated maleimide by thiol-ene reaction. HP-0 hydrogel pattern which is not biotinylated due to absence of maleimide is used as control and it was exposed to FITC-streptavidin. As expected, no significant fluorescence was observed due to minimal physiabsorption of streptavidin due to the bio-inert nature of the PEG-based hydrogel matrix (Figure 3.12a). Bioimmobilized hydrogel patterns with different amount of maleimide were observed by fluorescence microscope, fluorescence intensity was increased with the rise of thiol reactive maleimide in the gel (Figure 3.12 and Figure 3.13).

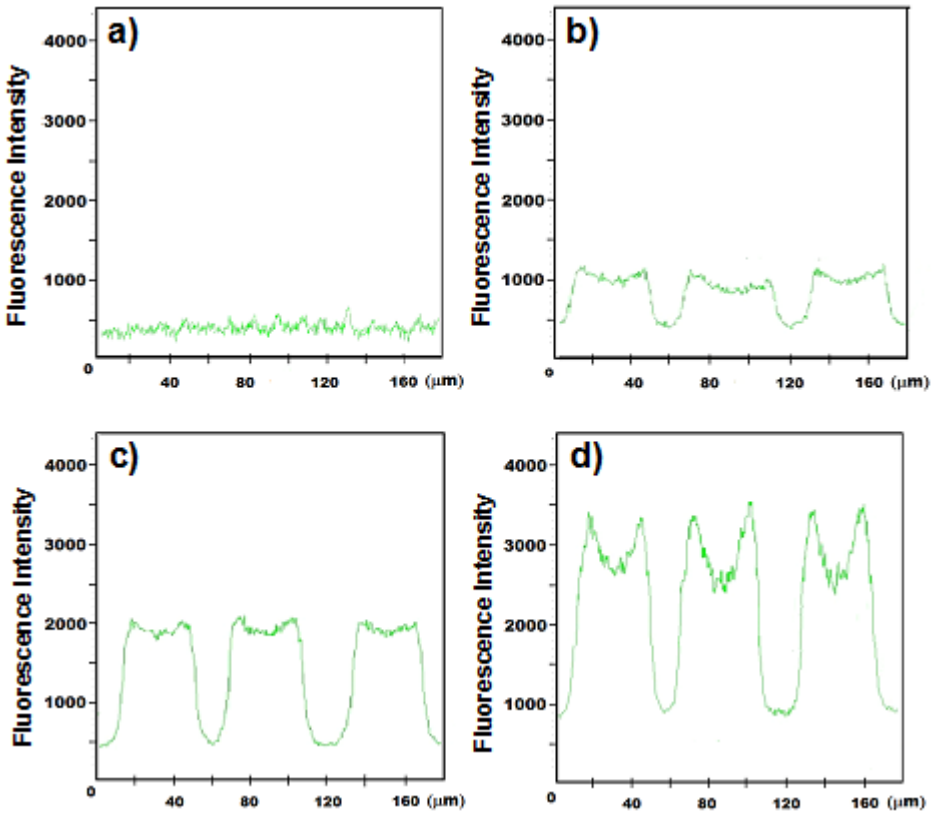

Figure 3.13. Fluorescence intensity profiles of BH-0 (a), BH-10 (b), BH-30 (c) and BH-60 (d).

4. EXPERIMENTAL

4.1. Materials

The furan protected maleimidyl methacrylate (FuMa-MA) monomer was synthesized according to previous report [27]. Poly (ethylene glycol) methyl ether methacrylate (PEGMEMA, M_w = 300) was purchased from Sigma Aldrich and purified by passing through the activated aluminum oxide column prior to use. Poly (ethylene glycol) diacrylate (PEG-DA, M_w = 700), 2,2-Dimethoxy-2-phenylacetophenone (DMPAP), 3-(trimethoxysilyl)propyl methacrylate (TMSPMA), 1-thioglycerol and triethylamine (TEA) were obtained from Sigma Aldrich and used without further purification. Methacryloyl chloride was obtained from Alfa Aesar and used as received. Biotinylated (triethylene glycol) undecanethiol (Biotin-SH) was obtained from Nanoscience Instruments (Phoenix, AZ). Fluorescein conjugated streptavidin (FITC-streptavidin) was obtained from Pierce and used as received. 4,4-Difluoro-1,3,5,7-tetramethyl-8-[(10-mercapto)]-4-bora-3a,4a-diaza-*s*-indacene (BODIPY-SH) was synthesized according to literature procedure [67]. HABA/Avidin reagent was obtained from Sigma. Other chemical reagents were obtained from commercial resources and were used as received. Dry solvents such as dichloromethane (DCM), tetrahydrofuran (THF) and toluene were obtained from SciMatCo purification system and other solvents were dried over molecular sieves. Column chromatography was performed using silica gel 60 (43-60 nm, Merck). Thin layer chromatography was performed using silica gel plates (Kieselgel 60 F254, 0.2 mm, Merck).

4.2. Fabrication of Photopolymerized Bulk-Hydrogel

Photopolymerized bulk-hydrogels were prepared by UV-initiated free radical photo polymerization at ambient temperature. Monomer mixtures were prepared by mixing of PEGMEMA as a monomer, PEG-DA as a crosslinker, DMPAP as a photoinitiator, DCM as a solvent with different feed amount of FuMa-MA monomer (BH-0, BH-10, BH-30, BH-60 in Table 1) into transparent glass vial. In order to check solvent effect for photopolymerization of hydrogel, photopolymerization of hydrogel containing 30% maleimide was performed in DCM and water/methanol (1:1, v/v) mixture, respectively.

Monomer mixture solutions were degassed with nitrogen and sonicated for 5 min at room temperature. The photopolymerization of bulk-hydrogel was carried by irradiating the monomer mixture under UV-light (254 nm, Scientific Instrument Co. Ltd) for 40 min at room temperature. UV lamp was placed at a distance of 3 cm from monomer mixture. The photopolymerized bulk-hydrogels were washed with THF several times to remove unreacted reactant and then dried by lyophilization for 12 hours. To determine monomer conversion, unreacted reactant in THF solutions were dried by reduced pressure and characterized by ^{1}H NMR (Figure 3.2). The protected FuMa-MA in bulk-hydrogel was activated as unprotected maleimide by retro-DA reaction. For the activation of gel, 0.2 g of hydrogel was deep into dry toluene and heated at 110°C under nitrogen for 12 h. The activated-hydrogel was precipitated into cold ether and dried under vacuum at room temperature overnight. Quantitative characterization of FuMa-MA in the bulk-hydrogel was done by thermogravimetric analysis (TGA).

4.3. Swelling Study of Bulk-Hydrogel

The lyophilized activated-hydrogel for 12 hr was cut into small pieces and weighted, mean weight was 35 ± 0.5 mg. Each hydrogel was placed into 25 mL beaker containing 10 mL deionized water at room temperature. At regular intervals the hydrogel was taken out of the beaker, surface moisture was removed by tissue paper, and then it was weighed. After this, the hydrogel was returned to the beaker and the water uptake was measured until the maximum mass was obtained. The percentage amount of water uptake (W_{up}) was calculated using the following equation

$$W_{up}(\%) = (W_{max} - W_{dry}) / W_{dry} \times 100 \quad (4.1)$$

where W_{max} is the maximum weight of the swollen hydrogel, W_{dry} is the weight of the dry hydrogel. All swelling studies were carried out in triplicate with different batches of similar hydrogels.

4.4. Modification of silicon wafer substrate with TMSPMA

Silicon wafer was cleaved into pieces that were approximately 1 cm^2, and then soaked in ‘piranha’ solution consisting of 3:1 ratio of H_2SO_4 and 30 % H_2O_2 solution for

20 min, quickly rinsed with deionized water several times, then with isopropyl alcohol and finally dried under vacuum at room temperature. Piranha solution can spontaneously explode upon contact with organic compounds, so extra attention is needed when using it. For promoting the covalent adhesion between the silicon surface and the hydrogel, the silicon surface was modified with TMSPMA. Silicon wafer was soaked in a 10% (by weight) solution of TMSPMA in dry toluene for 12 hours at room temperature. The modified wafer was washed several times in toluene and methanol and then dried under vacuum.

4.5. Preparation and Activation of Photo-polymerized Hydrogel Pattern

The photo polymerized hydrogel pattern (HP) on the silicon surface was performed by capillary-force lithography with PDMS stamp [68]. PDMS stamp was used to obtain three-dimensional structured hydrogel pattern. The PDMS stamp with patterned structure was obtained by using standard photolithography [36]. To prepare the photoresist mold, negative photoresist SU-8 was spin-coated on the silicon wafer at 500 rpm for 10 seconds and 3000 rpm for 30 seconds. After spinning process the photoresist was dried via a soft baking at 95^{o}C for 25 min. Substrate was exposed to UV-light (365 nm) with a power around 1 mW/cm^2 for 5 min and post baked at 95^{o}C for 12 min. The photoresist was developed with mr-Dev 600 and rinsed with isopropanol and dried under vacuum. The PDMS stamp was prepared by pouring PDMS into the photoresist mold and left to cure. Then PDMS stamp was peeled off from the mold and was ready for the patterning process. The prepared PDMS stamp was carefully placed on the surface of the TMSPMA modified silicon wafer. Monomer mixture was dropped at the one open ends of channel of PDMS stamp on the silicon wafer and the channel of PDMS was filled with monomer mixture by capillary action. Monomer mixture in PDMS channel on the silicon surface was placed under UV lamp at a distance of 3 cm and exposed to 254 nm UV-light for 40 min. The monomer mixtures were prepared in same feed ratio for bulk-hydrogel. After exposure to UV-light, PDMS stamp was taken off from the silicon surface and hydrogel patterns on the surface were washed with THF to remove any unreacted reactants. The deprotection of the FuMa-MA moieties on the hydrogel pattern were carried out via retro-DA reaction, pattern samples were heated under vacuum at 110°C for 30 min and cooled under nitrogen.

4.6. Streptavidin Immobilization on the Biotinylated HP

Biotinylated hydrogel pattern (bio-HP) was prepared by soaking activated-hydrogel pattern (act-HP) in 3 mg Biotin-SH in 2 mL MeOH solution for 12 h under nitrogen at room temperature. The bio-HP was washed several times with MeOH and FITC-Streptavidin (0.2 mg/mL PBS) was added directly to the bio-HP. After immobilization of streptavidin on the bio-HP for 30 min, FITC-streptavidin immobilized hydrogel pattern (strep-HP) was rinsed with water several times and fluorescence microscope images were taken. For control experiment, green-fluorescent BODIPY-SH dye was attached to act-HP contains maleimide and without maleimide samples to identify absence of thiol-reactive maleimide and physical entrapment of dye in the gel. The act-HP samples were incubated with a BODIPY-SH (1 mg) in 2 mL dry THF solution for 12 h and washed several times with THF. Streptavidin immobilized HP and BODIPY-SH attached HP were analyzed by fluorescence microscope.

4.7. HABA/Avidin Assay of Biotinylated Bulk-Hydrogel

HABA/Avidin assay was performed to determine the amount of biotin in the hydrogel, available for binding to streptavidin [66]. HABA/Avidin assay was monitored by UV-vis spectrophotometer absorbance at 500 nm for the HABA/Avidin reagent and for the solution after addition of biotinylated bulk-hydrogel. The calibration curve was obtained by measuring the change in UV absorbance upon the addition of free-biotin of known concentration sequentially into the HABA/Avidin reagent. The equivalent amount of free-biotin available on the biotinylated bulk-hydrogel was calculated by comparing the absorbance changes to the calibration curve.

4.8. Measurement and Characterization

The synthesized monomer was characterized by ^{1}H NMR spectroscopy (Varian Mercury-MX 400 Hz) and Fourier Transform Infrared (FTIR) spectroscopy (Thermo Scientific Nicolet 380 FT-IR spectrometer). LabConco lyophilizer was used to dry the hydrogels. Thermogravimetric analysis (TGA) was carried out with a TGA Q50 from TA

instruments at a heating sample from ambient temperature to 600°C at a rate of 10°C/min under a nitrogen flow (100 mL/min). Elemental analysis data were obtained from Thermo Electron S.p.A. FlashEA® 1112 Elemental Analyzer (CHNS separation column, PTFE; 2 m; 6 x 5 mm). To characterize the hydrogel morphology, scanning electron microscopy (SEM) observation was performed with a ESEM-FEG/EDAX Philips XL-30 (Philips, Eindhoven, The Netherlands) operating at 10 kV. Hydrogels swollen in water were lyophilized and immersed in liquid nitrogen and then broken prior to taking an image. UV-visible spectra of HABA/Avidin assay were collected on a TU-1880 UV-vis spectrophotometer. Fluorescence microscopy (HBO100 ZEISS Fluorescence Microscopy, Carl Zeiss Canada Ltd, Canada) was used to confirm the attachment of BODIPY-SH and FITC-streptavidin to hydrogel pattern (reflector = AF 488).

5. CONCLUSION

Bulk-hydrogels and hydrogel patterns containing various amounts of maleimide functional groups that are reactive toward thiol containing molecules are successfully synthesized by photopolymerization in presence of photoinitiator and PEG-DA. Efficient conversion of the furan protected maleimide groups into their deprotected reactive forms was monitored by TGA analysis of bulk-hydrogels. Water uptake of hydrogels is found to be dependent on the mass fraction of hydrophobic FuMA-MA in the hydrogel structure by swelling test. The maleimide containing hydrogel patterns were efficiently functionalized with fluorescent thiol containing dye, BODIPY-SH, and a thiol containing biotin ligand. The immobilization of FITC-streptavidin onto these biotinylated hydrogel patterns proves that functionalization of hydrogel patterns could be controlled by varying the density of maleimide groups in the hydrogel patterns.

REFERENCES

1. Hahn, M. S., J. S. Miller, and J. L. West, "Three-dimensional Biochemical and Biomechanical Patterning of Hydrogels for Guiding Cell Behavior", *Advanced Materials*, Vol. 18, pp. 2679-2684, 2006.

2. Hoffman, A. S., "Hydrogels for Biomedical Applications", *Advanced Drug Delivery Rev.*, Vol. 54, pp. 3-12, 2002.

3. Campoccia, D., P. Doherty, M. Radice, P. Brun, G. Abatangelo, and D. F. Williams, "Semisynthetic Resorbable Materials from Hyaluronan Esterification", *Biomaterials*, Vol.19, pp. 2101–2127, 1998.

4. Li, J., X. Li, X. Ni, X. Wang, H. Li, and K. W. Leong, "Self-assembled Supramolecular Sydrogels formed by Biodegradable PEO–PHB–PEO Triblock copolymers and α-Cyclodextrin for Controlled Drug Delivery", *Biomaterials,* Vol. 27, pp. 4132-4140, 2006.

5. Harada, A., J. Li, and M. Kamachi, "The Molecular Necklace: A Rotaxane Containing many α -Cyclodextrins", Nature, Vol. 356, pp. 325–327, 1992.

6. Vervoort, L., V. G. Mooter, P. Augustijns, and R. Kinget, "Inulin hydrogels. I. Dynamic and Equilibrium Swelling Properties", *International Journal of Pharmaceutics,* Vol. 172, pp. 127– 135, 1998.

7. Lu, Y., and P. S. Low, "Folate Mediated Delivery of Macromolecular Anticancer Therapeutic Agents", *Advanced Drug Delivery Reviews*, Vol. 54, pp. 675-693, 2002.

8. Hongchen, D., and K. Matyjaszewski, "One-Pot Synthesis of Robust Core/Shell Gold Nanoparticles", *Macromolecules*, Vol. 43, pp. 4623-4628, 2010.

9. Wei, H. L., Z. Yang, Y. Chen, H. J. Chu, J. Zhu, and Z. C. Li, "Characterization of N-vinyl-2-pyrrolidone-based Hydrogels Prepared by a Diels-Alder Click Reaction in Water", *European Polymer Journal*, Vol. 46, pp. 1032-1039, 2010.

10. Gupta, N., B. Lin, L. Campos, M. Dimitriou, S. Hikita, N. Treat, M.Tirrell, D. Clegg, E. Kramer, and C. Hawker, "A versatile Approach to High-throughput Microarrays using Thiol-ene Chemistry", *Nature Chemistry*, Vol. 2, pp. 138-145, 2008.

11. Martens, P., and K. Anseth, "Characterization of Hydrogels Formed from Acrylate Modified poly (vinyl alcohol) Macromers", *Polymer*, Vol. 41, pp. 7715-7722, 2000.

12. Quaglia, F., **"**Bioinspired Tissue Engineering: The Great Promise of Protein Delivery Technologies", *International Journal of Pharmaceutics*, Vol. 364, pp. 281– 297, 2008.

13. Moore, K., M. Macsween, and M. Shoichet, "Immobilized Concentration Gradients of Neurotrophic Factors Guide Neurite Outgrowth of Primary Neurons in Macroporous Scaffolds", *Tissue Engineering*, Vol. 12, pp. 267– 278, 2006.

14. DeLong, S. A., J. J. Moon, and J. L. West, "Covalently Immobilized Gradients of bFGF on Hydrogel Scaffolds for Directed Cell Migration", *Biomaterials*, Vol. 26, pp. 3227-3234, 2005.

15. Taite, L. J., M. L. Rowland, K. A. Ruffino, B. R. E. Smith, M. B. Lawrence, and J. L. West, "Bioactive Hydrogel Substrates: Probing Leukocyte Receptor–Ligand Interactions in Parallel Plate Flow Chamber Studies", *Annals of Biomedical Engineering*, Vol. 34, pp. 1705–1711, 2006.

16. Burdick, J. A., and K. S. Anseth, "Photoencapsulation of Osteoblasts in Injectable RGD-Modified PEG Hydrogels for Bone Tissue Engineering", *Biomaterials*, Vol. 23, pp. 4315– 4323, 2002.

17. Chauhan, G. S., S. C. Jaswal, and M. Verna, "Post Functionalization of Carboxymethylated Starch and Acrylonitrile based Networks through Amidoximation for use as Ion Sorbents", *Carbohydrate Polymers,* Vol. 66, pp. 435-443, 2006.

18. Kolb, H. C., M. G. Finn, and K. B. Sharpless, "Click Chemistry: Diverse Chemical Function from a Few Good Reactions", *Angewandte Chemie International Edition,* Vol. 40, 2004– 2021, 2001.

19. Ossipov, D. A., and J. Hilborn, "Poly(vinyl alcohol)-based hydrogels formed by "click chemistry", *Macromolecules,* Vol. 39, pp. 1709– 1718, 2006.

20. Malkoch, M., R. Vestberg, N. Gupta, L. Mespouille, P. Dubois, A. F. Mason, J. L. Hedrick, Q. Liao, C. W. Frank, K. Kingsbury, and C. J. Hawker, "Synthesis of Well-Defined Hydrogel Networks Using Click Chemistry", *Chemical Communications,* Vol. 2774– 2776, 2006.

21. Xu, X. D., C. S. Chen, Z. C. Wang, G. R. Wang, S. X. Cheng, X. Z. Zhang, and R. X. Zhuo, " "Click" Chemistry for *in situ* Formation of Thermoresponsive P(NIPAAm-*co*-HEMA)-based Hydrogels", *Journal of Polymer Science, Polymer Chemistry,* Vol. 46, pp. 5263– 5277, 2008.

22. Altin, H., I. Kosif, and R. Sanyal, "Fabrication of "Clickable" Hydrogels via Dendron−Polymer Conjugates", *Macromolecules,* Vol. 43, pp. 3801–3808, 2010.

23. Witter, A., and H. Tuppy, "N-(4-Dimethylamino)-3,5-Dinitrophenyl)maleimide: A Coloured Sulfhydryl Reagent: Isolation and Investigation of Cysteine-containing Peptides from Human and Bovine Serum Albumin", *Biochimica et Biophysica Acta,* Vol. *45*, pp. 429-442, 1960.

24. Bontempo, D., K. L. Heredia, B. A. Fish, and H. D. Maynard, "Cysteine-Reactive Polymers Synthesized by Atom Transfer Radical Polymerization for Conjugation

to Proteins", *Journal of American Chemical Society,* Vol. 126, pp 15372–15373, 2004.

25. Reddick, J. J., J. Cheng, and W. R. Roush, "Relative Rates of Michael Reactions of 2'-(phenethyl)thiol with Vinyl Sulfones, Vinyl Sulfonate Esters, and Vinyl Sulfonamides Relevant to Vinyl Sulfonyl Cysteine Protease Inhibitors", *Organic Letters*, Vol. 5, pp 1967-1970, 2003.

26. Houseman, B. T., E. S. Gawalt, and M. Mrksich, "Maleimide-Functionalized Self-Assembled Monolayers for the Preparation of Peptide and Carbohydrate Biochips", *Langmuir*, Vol. 19, pp 1522-1531, 2003.

27. Dispinar, T., R. Sanyal, and A. Sanyal, "A Diels-Alder/Retro Diels-Alder Strategy to Synthesize Polymers Bearing Maleimide Side Chains", *Journal of Polymer Science Part A: Polymer Chemistry,* Vol. 45, pp 4545 – 4551, 2007.

28. Sanyal, A. "Diels-Alder Cycloaddition-Cycloreversion: A Powerful Combo in Materials Design", *Macromolecular Chemistry and Physics,* Vol. 211, pp. 1417-1425, 2010.

29. Kosif, I., E. J. Park, R. Sanyal, and A. Sanyal, "Fabrication of Maleimide Containing Thiol Reactive Hydrogels via Diels−Alder/Retro-Diels−Alder Strategy", *Macromolecules,* Vol. 43, pp 4140-4148, 2010.

30. Kim, P., K. W. Kwon, M. C. Park, S. H. Lee, S. M. Kim, and K. Y. Suh, "Soft Lithography for Microfluidics: a Review", *Biochip Journal,* Vol. 2, pp. 1-11, 2008.

31. Qin, D., Y. Xia, and G. M. Whitesides, "Soft Lithography for Micro- and Nanoscale Patterning", *Nature Protocols* Vol. 5, pp. 491–502, 2010.

32. Weibel, D. B., W. R. DiLuzio, and G. M. Whitesides, "Microfabrication Meets Microbiology", *Nature Reviews Microbiology*, Vol. 5, pp. 209-228, 2007.

33. Linder, V., H. K. Wu, X. Y. Jiang, and G. M. Whitesides, “Rapid Prototyping of 2D Structures with Feature Sizes Larger than 8μm”, *Analitical Chemistry*, Vol. 75, pp. 2522–2527, 2003.

34. Losic, D., J. G. Mitchell, R. Lal, and N. H. Voelcker, “Rapid Fabrication of Micro- and Nanoscale Patterns by Replica Molding from Diatom Biosilica”, *Advancad Functional Materials,* Vol. 17, pp. 2439–2446, 2007.

35. Mayer, M., J. Yang, I. Gitlin, D. H. Gracias, and G. M. Whitesides, “Micropatterned Agarose Gels for Stamping Arrays of Proteins and Gradients of Proteins”, Proteomics, Vol. 4, pp. 2366–2376, 2004.

36. Mrksich,, M., L. E. Dike, J. Tien, D. E. Ingber, and G. M. Whitesides, “Using Microcontact Printing to Pattern the Attachment of Mammalian Cells to Self-Assembled Monolayers of Alkanethiolates on Transparent Films of Gold and Silver”, *Experimental Cell Research*, Vol. 235, pp. 305-313, 1997.

37. Jeon, N. L., R. G. Nuzzo, Y. Xia, M. Mrksich, and G. M. Whitesides, “Patterned Self-Assembled Monolayers Formed by Microcontact Printing Direct Selective Metalization by Chemical Vapor Deposition on Planar and Nonplanar Substrates”, *Langmuir*, Vol. *21, pp.* 3024-3026, 1995.

38. Hovis, J. S., G. Steven, and S. G Boxer, “Patterning and Composition Arrays of Supported Lipid Bilayers by Microcontact Printing”, *Langmuir*, Vol. 17, pp 3400–3405, 2001.

39. Bernard, A., J. P. Renault, B. Michel, H. R. Bosshard, and E. Delamarche, “Fabricating Arrays of Single Protein Molecules on Glass Using Microcontact Printing”, *Advanced Materials*, Vol. 12, pp. 1067-1070, 2003.

40. Lange, S. A., V. Benes, D. P. Kern, J. K. H. Hörber, A. Bernard, “Microcontact Printing of DNA Molecules”, *Analytical Chemicals*, Vol. 76, pp. 1641–1647, 2004.

41. Csucs, G., M. Roger, J. W. Lussi, M. Textor, and G. Danuser, "Microcontact Printing of Novel Co-Polymers in Combination with Proteins for Cell-Biological Applications", *Biomaterials*, Vol. 24, pp. 1713-1720, 2003.

42. Santhanam, V., and R. P. Andres, "Microcontact Printing of Uniform Nanoparticle Arrays", *Nano Letters*, Vol. 4, pp. 41–44, 2004.

43. Rozkiewicz, D. I., D. Dominik Janczewski, W. Verboom, B. J. Ravoo, N. David, and D. N. Reinhoudt, " ''Click" Chemistry by Microcontact Printing", *Angewandte Chemie International Edition*, Vol. 45, pp. 5292–5296, 2006.

44. Kim, E., Y. M. Xia, G. M. Whitesides, "Micromolding in Capillaries: Applications in Materials Science", *Journal Americal Chemical Society,* Vol. 118, pp. 5722-5731, 1996.

45. Chang, C. Y., S. Y. Yang, L. S. Huang, T. M. Jeng, "A Novel Method for Rapid Fabrication of Microlens Arrays Using Micro-Transfer Molding with Soft Mold", *Journal of Micromechanics and Microengineering,* Vol. 16, pp. 999-1005, 2006.

46. Borenstein, J. T., E. J. Weinberg, B. K. Orrick, C. Sundback, M. R. Kaazempur Mofrad, and J. P. Vacanti, "Microfabrication of Three-Dimensional Engineered Scaffolds", *Tissue Engineering*, Vol. 13, pp. 1837-1844, 2007.

47. Koh, W. G., and M. Pishko, "Photoreaction Injection Renewing of Biomaterial Microstructures", *Langmuir,* Vol. 19, pp. 10310-10316, 2003.

48. Lee, S. H., J. J. Moon, and J. L. West, "Three-Dimensional Micropatterning of Bioactive Hydrogels via Two-Photon Laser Scanning Photolithography for Guided 3D Cell Migration", *Biomaterials*, Vol. 29, pp. 2962-2968, 2008.

49. Tan, W., and A. T. Desai, "Microfluidic Patterning of Cells in Extracellular Matrix Biopolymers: Effects of Channel Size, Cell Type and Matrix Composition on Pattern Integrity", *Biomedical Microdevices,* Vol. 5, pp. 235-244, 2003.

50. Mironov, V., T. Boland, T. Trusk, G. Forgacs, and R. R. Markwald, "Organ Printing: Computer-Aided Jet-Based 3D Tissue Engineering", *Trends Biotechnology*, Vol. 21, pp. 157-161, 2003.

51. Langer, R., and D. A. Tirrell, "Designing Materials for Biology and Medicine", *Nature*, Vol. 428, pp. 487-492, 2004.

52. West J. L., and J. A. Hubbell, "Separation of the Arterial Wall from Blood Contact Using Hydrogel Barriers Reduces Intimal Thickening After Balloon Injury in the Rat: The Roles of Medial and Luminal Factors in Arterial Healing", *Proc. Natl. Acad. Sci. USA*, Vol. 93, pp. 13188–13193, 1996.

53. Sawhney, A. S., C. P. Pathak, J. J. van Rensburg, R. C. Dunn, and J. A. Hubbell, "Optimization of Photopolymerized Bioerodible Hydrogel Properties for Adhesion Prevention", *Journal of Biomedical Materials Reaserch*, Vol. 28, pp. 831-838, 1994.

54. Chowdhury, S. M., and J. A. Hubbell, "Adhesion Prevention with Ancrod Released via a Tissue-Adherent Hydrogel", *Journal of Surgery Reaserch*, Vol. 61, pp. 58-64, 1996.

55. Quinn, C. P., C. P. Pathak, A. Heller, and J. A. Hubbell, "Photo-Crosslinked Copolymers of 2-Hydroxyethyl Methacrylate, Poly(Ethylene Glycol) Tetra-Acrylate and Ethylene Dimethacrylate for Improving Biocompatibility of Biosensors", *Biomaterials*, Vol. 16, pp. 389-396, 1995.

56. Pathak, C. P., A. S. Sawhney, and J. A. Hubbell, "Rapid Photopolymerization of Immunoprotective Gels in Contact with Cells and Tissue", *Journal Americal Chemical Society*, Vol. 114, pp. 8311-8312, 1992.

57. Xia, Y., E. Kim, X. M. Zhao, J. A. Rogers, M. Prentiss, and G. M Whitesides, "Complex Optical Surfaces Formed by Replica Molding Against Elastomeric Masters", *Science*, Vol. 273, pp. 347-349, 1996.

58. Suh, K. Y., Y. S. Kim, and H. H. Lee, **"**Capillary Force Lithography", *Advanced Materials*, Vol.13, pp. 1386-1389, 2001.

59. Kim, E., Y. Xia, and G. M. Whitesides, "Polymer Microstructures Formed by Moulding in Capillaries", *Nature*, Vol. 376, pp. 581-584, 1995.

60. Marsden, D. M., R. L. Nicholson, M. Ladlow, and D. R. Spring, **"**3D Small Molecule Microarray", *Chemicals Communication*, Vol. 46, 7107-7109, 2009.

61. Bailey, G. C., and T. M. Swager, "Masked Michael Acceptors in Poly (phenyleneethynylene)s for Facile Conjugation", *Macromolecules,* Vol. 39, pp. 2815-2818, 2006.

62. Kang, G., Y. Cao, H. Zhao, and Q. Yuan, "Preparation and Characterization of Crosslinked Poly (Ethylene Glycol) Diacrylate Membranes with Excellent Antifouling and Solvent-Resistant Properties", *Journal of Membrane Science*, Vol. 318, pp. 227-232, 2008.

63. Lin, C., and A. T. Matters, "Hydrogels in Controlled Release Formulations: Network Design and Mathematical Modeling", *Advanced Drug Delivery Reviews*, Vol. 58, pp. 1379-1408, 2006.

64. Watkins, A. W., and K. S. Anseth, "Investigation of Molecular Transport and Distributions in Poly(ethylene glycol) Hydrogels with Confocal Laser Scanning Microscopy", M*acromolecules*, Vol. 38, pp. 1326-1334, 2005.

65. Colonne, M., Y. Chen, K. Wu, S. Freiberg, S. Giasson, and X. X. Zhu, "Binding of streptavidin", *Bioconjugate Chemistry*, Vol. 18, pp. 999-1003, 2007.

66. Qi, K., Q. G. Ma, E. E. Remsen, C. G. Clark, and K. L. Wooley, "Determination of the Bioavailability of Biotin Conjugated onto Shell Cross-Linked (SCK) Nanoparticles", *Journal Americal Chemical Society*, Vol. 126, pp. 6599-6607, 2004.

67. Shepherd, J. L., A. Kell, E. Chung, C. W. Sinclar, M. S. Workentin, and D. Bizzotto, "Selective Reductive Desorption of a SAM-Coated Gold Electrode Revealed Using Fluorescence Microscopy", *Journal Americal Chemical Society*, Vol. 126, pp. 8329-8335, 2004.

68. Suh, K. Y., and H. H. Lee, "Capillary Force Lithography: Large-Area Patterning, Self-Organization and Anisotropic Dewetting", *Advanced Functional Materials*, Vol. 12, pp. 405-413, 2002.